PROCESSING & CHARACTERIZATION OF NICKEL – ALUMINIDE COATING ON METAL SUBSTRATES

A THESIS SUBMITTED IN PARTIAL FULFILMENT OF THE REQUIREMENTS FOR THE DEGREE OF

Master of Technology

in

Mechanical Engineering

By

M. CHAITHANYA

Department of Mechanical Engineering

National Institute of Technology

Rourkela

MAY, 2007

PROCESSING & CHARACTERIZATION OF NICKEL – ALUMINIDE COATING ON METAL SUBSTRATES

A THESIS SUBMITTED IN PARTIAL FULFILMENT OF THE REQUIREMENTS FOR THE DEGREE OF

Master of Technology
in
Mechanical Engineering

[Specialization: Production Engineering]

By

M. CHAITHANYA

Under the Guidance of

Dr. Alok Satapathy
Department of Mechanical Engineering
&
Dr. S.C.Mishra
Department of Metallurgical & Materials Engineering

Department of Mechanical Engineering
National Institute of Technology
Rourkela

May, 2007

National Institute of Technology
Rourkela

CERTIFICATE

This is to certify that the thesis entitled **" PROCESSING AND CHARACTERIZATION OF NICKEL – ALUMINIDE COATING ON METAL SUBSTRATES "** submitted by **Sri M. Chaithanya** in partial fulfillment of the requirements for the award of Master of Technology degree in Mechanical Engineering with specialization in Production Engineering to the National Institute of Technology, Rourkela (Deemed University) is an authentic work carried out by him under our supervision and guidance.

To the best of our knowledge, the matter embodied in the thesis has not been submitted to any other University / Institute for the award of any Degree or Diploma.

Dr. S.C.Mishra
Dept. of Mett. & Materials Engg.
National Institute of Technology
Rourkela 769008

Dr. Alok Satapathy
Dept. of Mechanical Engg.
National Institute of Technology
Rourkela 769008

ACKNOWLEDGEMENT

It gives me immense pleasure to express my deep sense of gratitude to my guides **Dr. Alok Satapathy**, Asst. Professor, Department of Mechanical Engg. and **Dr. S.C. Mishra**, Asst.Professor, Department of Metallurgical & Materials Engineering for their invaluable guidance, motivation and constant inspiration. I am thankful to both of them for suggesting the problem for my M. Tech project wok.

I wish to record my sincere thanks to **Dr. P.V.Ananthapadmanabhan** and **Mr. K.P.Sreekumar**, Sr. Scientists at the Laser and Plasma Technology Division, B.A.R.C. Mumbai for guiding me in preparing the coatings using a plasma spray system for this work.

I am extremely thankful to **Prof. B. K. Nanda**, Head, Department of Mechanical Engineering and **Prof. K. P. Maity**, Course Coordinator for their help and advice during the course of this work.

My friends and class mates **Sri Nagamahendra Babu** , **Mrs. Rojaleena Das** and **Ms. Anupama Sahoo** deserve my special thanks for their help and support throughout this work.

I am also thankful to all my well wishers, class mates and friends for their inspiration and help.

Date: **M.Chaithanya**

Roll No. 20503044

CONTENTS

****

ABSTRACT

Nickel-aluminide has drawn enormous attention because of its technological and scientific interest. It has long been used as a coating material on industrial and structural elements, where its function has been to minimize the thermo-mechanical stresses at the substrate-coating interface and to promote coating adhesion. Its role, therefore, has mostly been restricted as a bond coat between the core component and the ceramic top coat. Its use as a top coat material has not been reported so far.

The present research work focuses on the study of nickel-aluminide deposition as the top coat on metallic substrate without any intermediate bond coat. Mild steel and copper are chosen as the substrate material and the deposition of Ni-Al is made by atmospheric plasma spray coating route. The basic aim has been to study the formation of Ni-Al coatings and to characterize them. They are characterized for their hardness, porosity, adhesion strength and microstructure. The significant phase changes/ transformations taking place during with the plasma spraying are studied. In addition, the coating deposition efficiencies at various operating conditions are also evaluated. A qualitative analysis of the experimental results with regard to coating deposition efficiency is made and a prediction model using neural computation is proposed. The ability of these coatings to combat solid particle erosion wear is assessed.

It is found that mixture of commercial grade nickel and aluminum powder is coatable on metal substrates by thermal plasma spraying technique. These coatings possess desirable coating characteristics such as good adhesion strength, hardness and reasonable porosity etc. During plasma spray deposition, formation of aluminide phases of nickel is observed. Maximum adhesion strength of ~ 12.5 MPa is recorded for these nickel-aluminide coatings on mild steel substrates and ~ 10.15 MPa on copper substrates, at 20kW operating power level of plasma torch. Maximum deposition efficiency of ~ 57% is obtained for Ni-Al coatings on copper and ~ 54% on

mild steel substrates. Input power to the torch influences the coating adhesion strength, deposition efficiency and the coating hardness to a great extent. The coating morphology is also largely affected by the torch input power. Occurrence of phase transformations and formation of aluminide phases such as Ni_3Al, Ni_3Al_2 during plasma spraying is evident. The different aluminide phases observed in XRD studies corroborate to the observation of different hardness values of different optically distinguished phases. The coatings are harder than that of the substrate materials; and hence can be recommended for various tribological applications. The solid particle erosion wear resistance of these coatings is fairly good. The rate of erosion of the coating is found to be greatly affected by the angle of impact and the velocity of impact of the eroding particles.

Artificial neural networks can be gainfully employed to simulate property-parameter correlations of the coatings beyond the experimentation range. The ANN technique can also be used for prediction of coating performance under different operational conditions. The simulation can be extended to a parameter space larger than the domain of experimentation.

*****

LIST OF FIGURES

LIST OF TABLES

Chapter 1

INTRODUCTION

CHAPTER 1

INTRODUCTION

BACKGROUND

The incessant quest for higher efficiency and productivity across the entire spectrum of manufacturing and engineering industries has ensured that most modern-day components are subjected to increasingly harsh environments during routine operation. Critical industrial components are, therefore, prone to more rapid degradation as the parts fail to withstand the rigors of aggressive operating conditions and this has been taking a heavy toll of industry's economy. In an overwhelmingly large number of cases, the accelerated deterioration of parts and their eventual failure has been traced to material damage brought about by hostile environments and also by high relative motion between mating surfaces, corrosive media, extreme temperatures and cyclic stresses. Simultaneously, research efforts focused on the development of new materials for fabrication are beginning to yield diminishing returns and it appears unlikely that any significant advances in terms of component performance and durability can be made only through development of new alloys.

As a result of the above, the concept of incorporating engineered surfaces capable of combating the accompanying degradation phenomena like wear, corrosion and fatigue to improve component performance, reliability and durability has gained increasing acceptance in recent years. The recognition that a vast majority of engineering components fail catastrophically in service through surface related phenomena has further fuelled this approach and led to the development of the broad interdisciplinary area of surface modifications. A protective coating deposited to act as a barrier between the surfaces of the component and the aggressive environment that it is exposed to during operation is now globally acknowledged to be an attractive means to significantly reduce/suppress damage to the actual component by acting as the first line of defense.

Surface modification is a generic term now applied to a large field of diverse technologies that can be gainfully harnessed to achieve increased reliability and enhanced performance of industrial components. The increasing utility and industrial adoption of surface engineering is a consequence of the significant recent advances in the field. Very rapid strides have been made on all fronts of science, processing, control, modeling, application developments etc. and this has made it an invaluable tool that is now being increasingly considered to be an integral part of component design. Surface modification today is best defined as "the design of substrate and surface together as a system to give a cost effective performance enhancement, of which neither is capable on its own". The development of a suitable high performance coating on a component fabricated using an appropriate high mechanical strength metal/alloy offers a promising method of meeting both the bulk and surface property requirements of virtually all imagined applications. The newer surfacing techniques, along with the traditional ones, are eminently suited to modify a wide range of engineering properties. The properties that can be modified by adopting the surface engineering approach include tribological, mechanical, thermo-mechanical, electrochemical, optical, electrical, electronic, magnetic/acoustic and biocompatible properties.

The development of surface engineering has been dynamic largely on account of the fact that it is a discipline of science and technology that is being increasingly relied upon to meet all the key modern day technological requirements: material savings, enhanced efficiencies, environmental friendliness etc. The overall utility of the surface engineering approach is further augmented by the fact that modifications to the component surface can be metallurgical, mechanical, chemical or physical. At the same time, the engineered surface can span at least five orders of magnitude in thickness and three orders of magnitude in hardness.

Driven by technological need and fuelled by exciting possibilities, novel methods for applying coatings, improvements in existing methods and new applications have proliferated in recent years. Surface modification technologies have grown rapidly, both in terms of finding better solutions and in the number of technology variants available, to offer a wide range of quality and cost. The significant increase in the availability of coating process of wide ranging complexity that are capable of depositing a plethora of coatings and handling components of diverse geometry today, ensures that components of all imaginable shape and size can be coated economically.

Existing surface treatment processes fall under three broad categories:

(a) Overlay Coatings: This category incorporates a very wide variety of coating processes wherein a material different from the bulk is deposited on the substrate. The coating is distinct from the substrate in the as-coated condition and there exists a clear boundary at the substrate/coating interface. The adhesion of the coating to the substrate is a major issue.

(b) Diffusion Coatings: Chemical interaction of the coating-forming element(s) with the substrate by diffusion is involved in this category. New elements are diffused into the substrate surface, usually at elevated temperatures so that the composition and properties of outer layers are changed as compared to those of the bulk.

(c) Thermal or Mechanical Modifications of Surfaces: In this case, the existing metallurgy of the component surface is changed in the near-surface region either by thermal or mechanical means, usually to increase its hardness. The type of coating to be provided depends on the application. There are many techniques available, e.g. electroplating, vapour depositions, thermal spraying etc. Of all these techniques, thermal spraying is popular for its wide range of applicability, adhesion of coating with the substrate and durability. It has gradually emerged as the most industrially useful method of developing a variety of coatings, to enhance the quality of new components as well as to reclaim worn/wrongly machined parts.

The type of thermal spraying depends on the type of heat source employed and consequently flame spraying (FS), high velocity oxy-fuel spraying (HVOF), plasma spraying (PS) etc. come under the umbrella of thermal spraying. Plasma spraying utilizes the exotic properties of the plasma medium to impart new functional properties to conventional and non-conventional materials and is considered as one highly versatile and technologically sophisticated thermal spraying technique. It is a very large industry with applications in corrosion, abrasion and temperature resistant coatings and the production of monolithic and near net shapes [**1**]. The process can be applied to coat on variety of substrates of complicated shape and size using metallic, ceramic and /or polymeric consumables. The production rate of the process is very high and the coating adhesion is also adequate. Since the process is almost material independent, it has a very wide range of applicability, e.g., as thermal barrier coating, wear resistant coating etc. Thermal barrier coatings are provided to protect the base material, e.g., internal combustion engines , gas turbines etc. at elevated temperatures. Zirconia (ZrO_2) is a conventional thermal barrier coating material. As the name suggests, wear resistant coatings are used to combat wear especially in cylinder liners, pistons, valves,

spindles, textile mill rollers etc. Some ceramics like alumina (Al_2O_3) ,titania (TiO_2) and zirconia (ZrO_2) are some of the conventional wear resistant coating materials [**2**]. Apart from ceramics, a number of metallic and inter-metallic coatings are also in use to protect the core of the engineering and/or structural components.

Inter-metallic compounds find extensive use in high temperature structural applications [**3-6**].In particular, nickel-aluminm alloys and their derivatives have potential demand in aero space industry and other high performance applications.

SCOPE OF THE THESIS

The basic aim of the present work is to study the formation of Ni-Al coatings and to characterize them. Coatings are deposited on mild steel and copper substrates by plasma spraying technique. They are characterized for their hardness, porosity, adhesion strength and microstructure. The significant phase changes/ transformations taking place during with the plasma spraying are studied. In addition, the coating deposition efficiencies at various operating conditions are also evaluated. A qualitative analysis of the experimental results with regard to coating deposition efficiency using statistical techniques is made. The ability of these coatings to combat solid particle erosion wear is assessed.

****

Chapter 2

LITERATURE SURVEY

CHAPTER 2

LITERATURE SURVEY

This chapter deals with the literature survey of the broad topic of interest namely the development of surface modification technology for tribological applications. This treatise embraces various coating techniques with a special reference to plasma spraying, the coating materials and their characteristics. It also presents a brief review of previous work reported on nickel-aluminide and other inter-metallic coatings.

At the end of the chapter a summary of the literature survey and the knowledge gap in the earlier investigations are presented. The objectives of the present work are also outlined.

SURFACE MODIFICATION

Surface modification is a relatively new term that has come up in the last two decades or so to describe interdisciplinary activities aimed at tailoring the surface properties of engineering materials. The object of surface engineering is to upgrade their functional capabilities keeping the economic factors in mind [**7**]. *Surface Engineering* is the name of the discipline - *surface modification* is the philosophy behind it. To elucidate the matter an example can be taken. Tungsten carbide cobalt composite is a very popular cutting tool material, and is well known for its high hardness and wear resistance. If a thin coating of TiN is applied on to the WC-Co insert, its capabilities increase considerably [**8**]. Actually a cutting tool, in action, is subjected to a high degree of abrasion, and TiN is more capable of combating abrasion. On the other hand, TiN is extremely brittle, but the relatively tough core of WC-Co composite protects it from fracture. Thus through a surface modification process we assemble two (or more) materials by the appropriate method and exploit the qualities of both [**9, 10**]. It is a very versatile tool for technological development provided it is applied judiciously keeping the following restrictions in mind:

(i) The technological value addition should justify the cost, and

(ii) The choice of technique must be technologically appropriate.

TECHNIQUES OF SURFACE MODIFICATION

Today a large number of commercially available technologies are present in the industrial scenario and figure 2.1 exhibits some of them [**9**]. An overview of such technologies is presented below.

Plating

Amongst plating processes, electroplating is quite popular. The substrate (necessarily conducting) forms an electrode (cathode) and is submerged in an appropriate electrolyte [**11**]. As current passes through the electrolytic cell, ions of plating material emerge from the electrolyte and deposit on to the cathode (the substrate). In electroless plating, deposition occurs by catalytic reduction of the solute present in the plating bath. Electrochemical conversion coating appears on the surface of the substrate (which acts as an electrode) as a result of a chemical reaction between the electrolyte and the surface. For example in presence of H_2SO_4 (electrolyte) the top layer of aluminium (electrode) is oxidized to form aluminium oxide [**12**]. Electroforming is the process of electro- depositing a material on a removable mandrel to make a part. Plating can be used for modification of physical, mechanical or corrosion properties [**13**].

Plating techniques cater to a large number of materials. A composite coating with non-conducting materials like diamond is also possible by plating. It caters to wear, corrosion, rebuilding and electrical applications. Some of the processes are capable of providing uniform coating throughout the surface even in deep holes and re-entrant corners (electroless plating). Selective areas of a surface can be plated too [**12,14,15**].

But electroplating is prone to metallurgical embrittlement and provides only moderate adhesion where as electroless plating is quite slow [**11,16**].

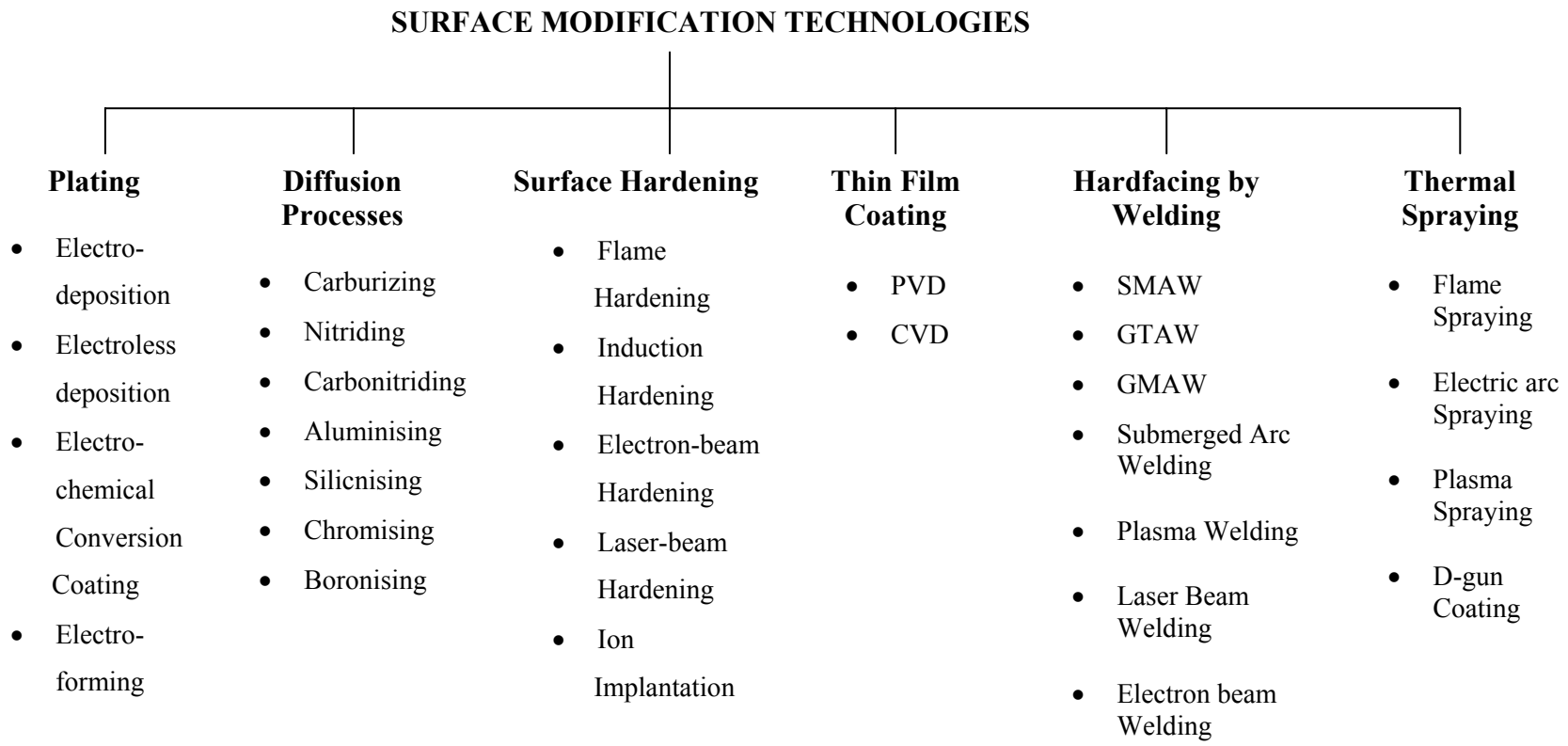

Fig. 2.1 Various forms of surface modification technologies

Diffusion Processes

As the name suggests, the process involves the diffusion of an element into the substrate matrix [**17**]. The process is normally conducted at an elevated temperature to promote diffusion. The diffusing species create a layer on the substrate and the properties of that layer are modified. The elements used as diffusing species are carbon, nitrogen, aluminium, chromium, silicon, boron, etc. The choice of the diffusing species depends on applications, but carbon and nitrogen are the two most widely used elements and the processes are known as carburising and nitriding respectively [**18**]. Both processes are normally carried out on steel substrates. The substrate is kept in an environment rich in carbon or nitrogen. At a high temperature, the elements slowly diffuse into the substrates owing to the concentration gradient. Carburising enriches the carbon content of the substrate case and upon quenching the case layer hardens owing to the martensitic transformation. Nitriding also creates a very hard layer on the substrate surface. Here hardening occurs owing to a solid solution strengthening. These two processes are mainly used for wear applications and so are boronising and carbo-nitriding. Chromising, siliconising, and aluminising on the other hand are for corrosion /oxidation resistance applications [**19,20**] .

But diffusion processes have certain limitations as well. They cannot cater to applications like rebuilding. Some processes often create distortion (case carburising). Some of the processes are very slow and the case depth obtained is limited (gas carburising). Some of the processes are carried out in aggressive environment (salt nitriding) with potential environmental hazard. Applications are limited to metals only.

Surface Hardening

The process involves heating a component surface (or part of it) beyond a critical temperature and quickly cooling it by quenching to induce martensitic transformation. The process is restricted to cast iron and steels. Here a heat source for raising the temperature of the work piece is needed. The process is named after the heat source used and typical examples are flame hardening (oxy-acetylene flame), induction hardening (induction heating), laser hardening (laser beam), electron beam hardening (electron beam) etc. [**21**] . The carbon content of the work piece must be at least 0.6%, otherwise martensitic transformation may not occur. Except for the ion implantation process, these processes do not involve any

material addition. In the ion implantation process, suitable materials are taken in ion form and they are directed at the surface to be implanted on. These processes are utilized to develop a hard case of low thickness, while retaining the softness of the core [**22**].

A small part of a big component can be hardened (flame hardening) and no material addition is required. Adhesion does not impose any restriction, since the hardened layer is an integral part of the original component. But the process is restricted to ferrous materials. Sometime the process is prone to distortion. Some of the processes require highly skilled manpower (e.g., flame hardening). Except for flame hardening, the set-up cost is high for all other processes.

Thin Film Coating

In this process a thin layer of a pure element or a compound can be deposited on substrate [9]. This technique can be broadly classified into two categories:

- Physical vapour deposition,
- Chemical vapour deposition

Physical Vapour Deposition (PVD)

This process is carried out in an evacuated chamber. The target (substrate) and the coating material are kept facing each other. The coating material is heated using a heat source like electrical heater or electron beam, in low pressure. The coating material evaporates directly from solid state and deposits on the target. This is known as thermal evaporation [**23**]. In another process, known as sputter coating [**24**], the target and coating materials are connected to two electrodes (anode and cathode, respectively) of a suitable power supply and an inert gas is released in the space between them. The gas undergoes ionization in the electric field. The positive ions rush towards the cathode (i.e., the coating material) and dislodge ions from it. These ions move toward the anode and deposit on the target. Ion plating is a combination of these two processes where the coating material is heated and at the same time a gas plasma is created to expedite the process [**25**].

Using this process pure elements as well as compounds can be deposited. It is quite simple, involves low cost equipment and addresses many fields of applications, e.g., electronic, electrical, wear, etc. This is a line of sight process, and therefore parts having complicated shape may not be coated. Since it is conducted in vacuum, large parts cannot be coated [**9**].

Chemical Vapour Deposition (CVD)

The material to be coated is kept in an evacuated chamber equipped with the facility of electrical heating. After the substrate is heated to the required temperature, the appropriate gases are introduced into the reactor for chemical reaction in contact with the hot substrate. One of the reaction products is a solid, which deposits on the substrate surface. The residual gases are taken out of the chamber [**26**].

Intricate shapes can be coated by this technique. Rate of deposition is higher than PVD. Certain items can be deposited using CVD only. But since it is carried out at a high temperature (700°C or above), thermal damages may come into play. Set up is more complicated than PVD [**27**].

Hard facing by Welding

Welding conventionally is a process of joining two metallic parts. Shield Metal Arc Welding (SMAW) is the most common welding process. Here the base metals are kept close to each other and an electric arc is created between the base metal (near the junction) and the consumable electrode. As a result both the consumable electrode (filler material) and the edge of the base metal melt. The filler material of the electrode transfers to the molten weld pool and upon freezing of such pool a solid weld bead is formed. The strength of the weldment is supposed to be greater than that of the base material [**28**]. In the case of the hard facing, the filler material is deposited onto the base material to form a metallurgically bonded second layer. Now the first layer of the deposit is diluted by the diffusion of the base material constituents into it. Normally a second layer is also deposited at the top of the first one. In welding either similar or otherwise compatible filler material are normally used for the joining purpose. Alloyed electrodes, with a tailored composition to suit particular situations of surfacing, are also used [**29**]. There are many techniques of welding and are shown in Figure 2.1. Each has its own application domain.

Strongest possible bonding is obtained in this process. All weldable metals and alloys can be used. It can be carried out with low cost equipment. A thick layer can be built up rapidly. The process can be entirely automated. But this technique is restricted to metallic materials. Products are vulnerable to residual stress related distortion. The hard faced layer may undergo dilution by the diffusion of base material constituents. Products may require a post-weld finishing operation in many applications [**28, 30**].

Thermal Spraying

It is the generic category of material processing technique that apply consumables in the form of a finely divided molten or semi molten droplets to produce a coating onto

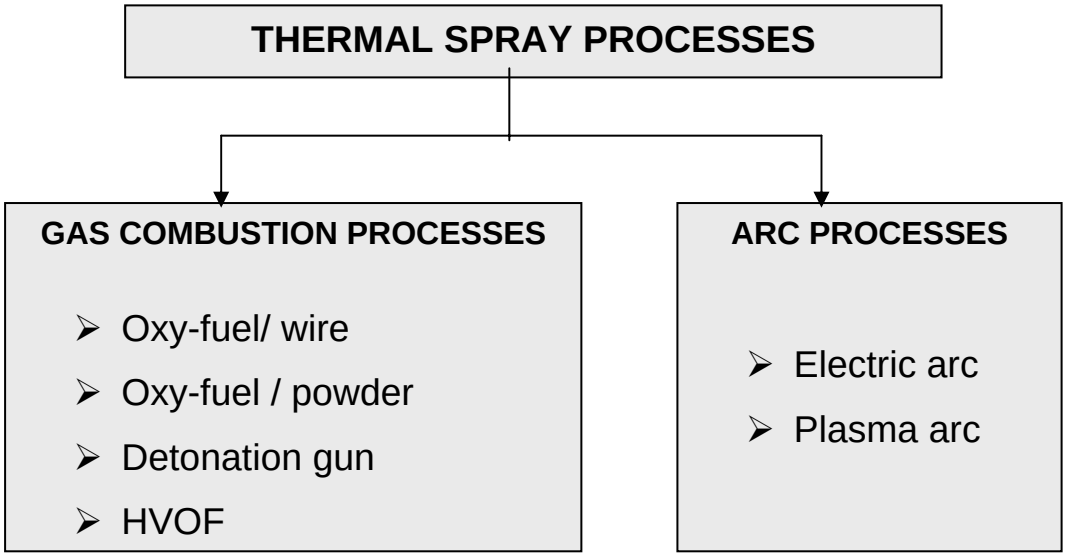

Fig. 2.2 Categorization of common thermal spray processes

the substrate kept in front of the impinging jet. The melting of the consumables may be accomplished in a number of ways, and the consumable can be introduced into the heat source in wire or powder form. Thermal spray consumables can be metallic, ceramic or polymeric substances. Any material can be sprayed as long as it can be melted by the heat source employed and does not undergo degradation during heating [**28 , 31**]. The nature of bonding at the coating-substrate interface is not completely understood. It is normally assumed that bonding occurs by the mechanical interlocking. Under this circumstance it is generally possible to ignore the metallurgical compatibility [**9**]. This is an extremely

significant feature of thermal spraying. Another interesting aspect of thermal spraying is that the surface temperature seldom exceeds 200^0 C. Hard metal or ceramic coating can be applied to thermosetting plastics. Stress related distortion problems are also not so significant. The spraying action is achieved by the rapid expansion of combustion gases (which transfer the momentum to the molten droplets) or by a separate supply of compressed air.
There are two basic ways of generating heat required for melting the consumables, [31, 32]

(i) Combustion of a fuel gas
(ii) High energy electric arc

Figure 2.2 shows the common thermal spray processes fitting into the above mentioned categories. The processes mentioned above are discussed briefly in the following articles but plasma spraying has been discussed separately.

Flame Spraying with Wire

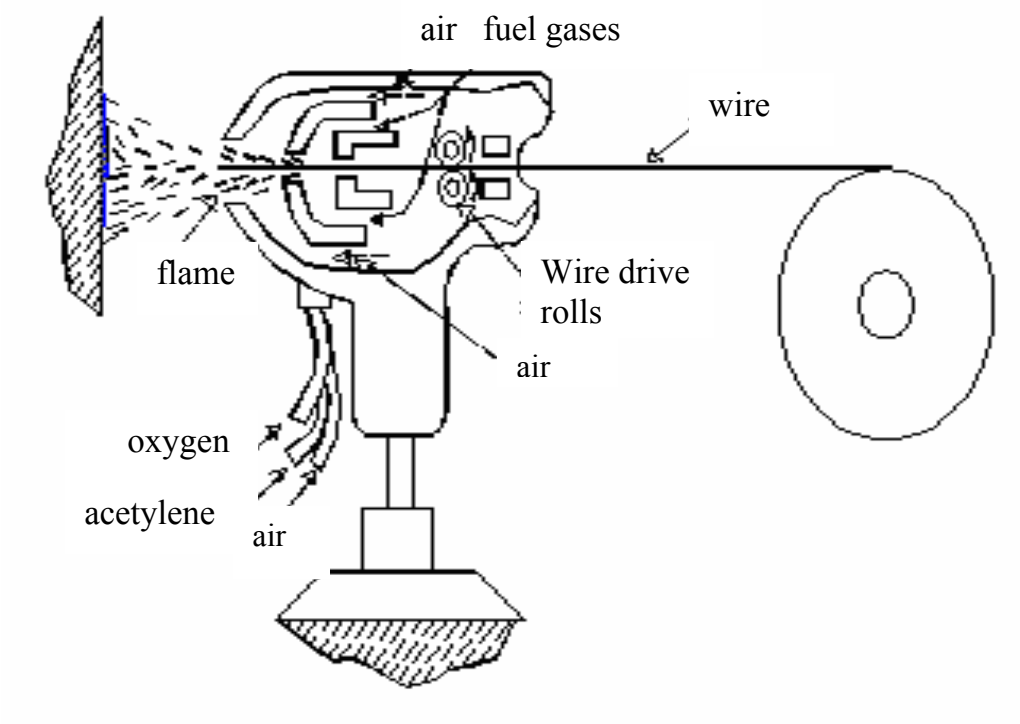

Fig. 2.3 Arrangement for the wire flame spraying

The arrangement is shown in figure 2.3, and the set-up consists of a spraying gun, a wire feeding arrangement, oxygen and acetylene gas cylinders and an air compressor [**9**]. A proportionate mixture of oxygen and acetylene is taken inside a chamber located.

The set up cost for flame spraying is quite low. Thick metallic layer can be deposited easily and hence it is quite useful for rebuilding purpose. But it is applicable to metallic materials only.

Flame Spraying with Powder

The arrangement is shown in Figure 2.4. The process is carried out with a gun in which facility for fuel gas (oxy-acetylene) injection and powder storage are integrated. The flame is kept at a convenient distance from the substrate. The consumable-powders are kept inside the hopper integrated with the gun and can be released to the flame by the action of a trigger. The powder is gravity fed to the flame; it melts and deposits on to the substrate to form a coating. In some cases the flame is taken close to the coating immediately after deposition for further melting. In this case the bond strength achieved is higher, but the temperature of the substrate increases considerably [**9,31, 32**].

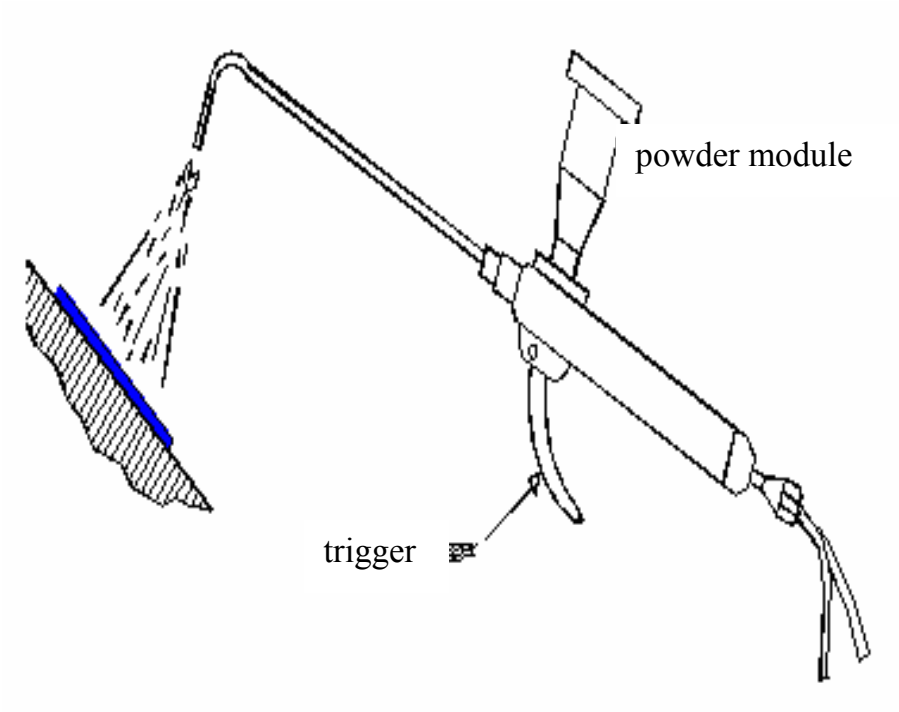

Fig. 2.4 Arrangement for the flame spraying with powders

The equipment cost is low. A large number of alloys (even cermets) are available in powder form. But ceramic materials cannot be deposited by this method. The deposition rate is very slow.

Detonation Gun Coating

This is a proprietary coating process. The basic set up is shown in Figure 2.5.

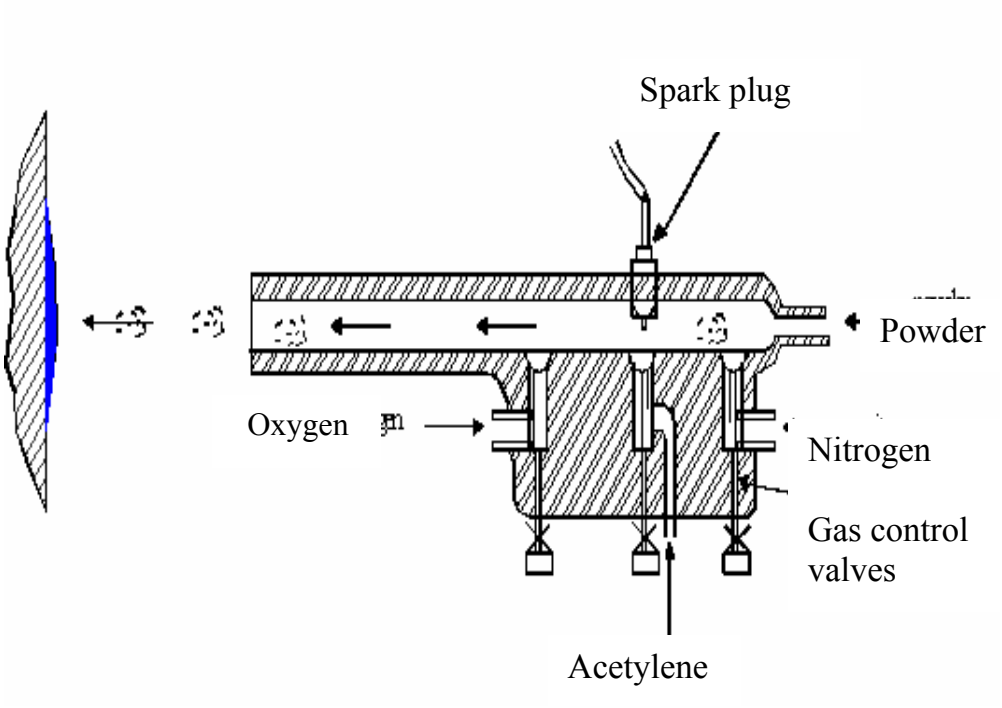

Fig. 2.5 Arrangement for the D-gun coating

Consumable powder is fed into the gun under a small gas pressure. Valves are opened to allow oxygen and acetylene to enter the combustion chamber of the gun. The mixture is then detonated by the sparks from spark plugs and an explosion occurs immediately. The temperature of the detonation fuel is about 3800^0 C, and it is a sufficiently high temperature to melt most of the materials. Immediately after the detonation, hot particles (undergoing melting) rush toward the target at a very high velocity. This factor is very important for having a well-bonded, dense coating. Detonation cycles are repeated four to eight times per second and nitrogen gas is used to flush out the combustion products after each cycle. This process produces very loud noise, and therefore the spraying is conducted inside a sound proof room. It also requires an elaborate arrangement for fuel and purge gas control, powder feeding, gun cooling and spark plug operation [**9, 31, 32**]. Using this technique metals, alloys and ceramics can be melted .Well bonded and dense coating can be produced. But the process is expensive and involves very elaborate arrangement. The process also produces loud noise.

High Velocity Oxy-Fuel Spraying (HVOF)

The arrangement is shown in Figure 2.6. Oxygen and fuel gas (propylene or hydrogen) mixture is introduced in the combustion chamber of the gun. It lights into a flame when ignited and the burnt gas acquires a very high temperature and escapes from the confinement of the small chamber at a high velocity in the process of expansion. The flame is at right angle to the muzzle of the gun. From one end of the gun, powder is fed in the center of the flame by a carrier gas. The particles melt and are immediately carried to the target by the gas, escaping at a very high velocity through the nozzle of the gun [**35, 36, 37**] .

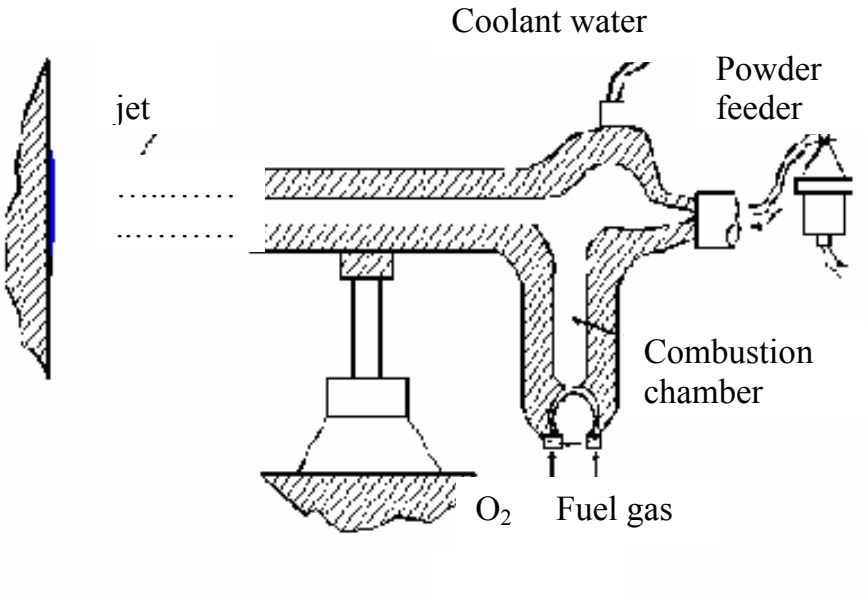

Fig. 2.6 Arrangement for the HVOF spraying

Advantages of this spraying technique include good substrate-coating adhesion, high coating density. It is applicable to both metals and ceramics. It involves less set up cost as compared to plasma or detonation gun.

Electric Arc Spraying

The arrangement is shown in Figure 2.7. An electric arc is created between the tips of two conducting wires. The heat produced melts the tips and these molten tips are dislodged and directed to a target by a compressed air jet. The wires are fed by the independent wire feed mechanisms. Electric power is supplied by a rugged welding power supply. The process is capable of spraying at a very high deposition rate [**9, 38**]. The set up for electric arc spraying

is simple and cheap. But only conducting materials can be sprayed. The substrate-coating adhesion and density is not comparable to plasma spraying or detonation gun.

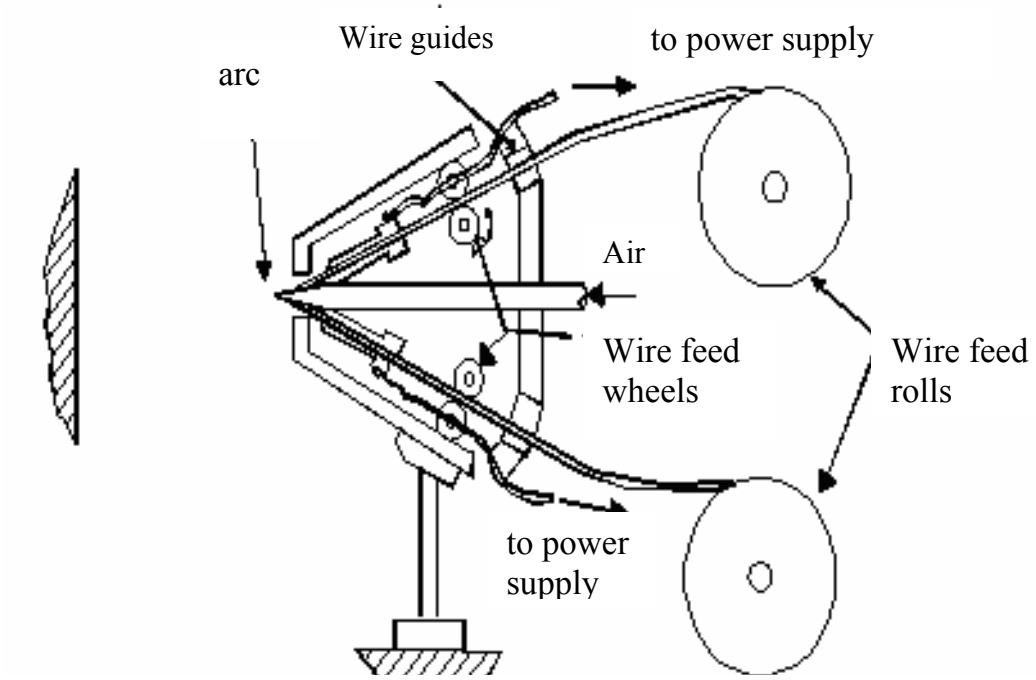

Fig. 2.7 Arrangement for the electric arc spraying

Plasma Spraying

Plasma spraying is the most versatile thermal spraying process and the general arrangement is shown in Figure 2.8. An arc is created between tungsten tipped copper cathode and an annular copper anode (both water cooled). Plasma generating gas is forced to pass through the annular space between the electrodes. While passing through the arc, the gas undergoes ionization in the high temperature environment resulting plasma. The ionization is achieved by collisions of electrons of the arc with the neutral molecules of the gas. The plasma protrudes out of the electrode encasement in the form of a flame. The consumable material, in the powdered form, is poured into the flame in metered quantity. The powders melt immediately and absorb the momentum of the expanding gas and rush towards the target to form a thin deposited layer. The next layer deposits onto the first immediately after, and thus the coating builds up layer by layer [**7, 9, 28, 34**]. The temperature in the plasma arc can be as high as $10{,}000^0$C and it is capable of melting anything. Elaborate cooling arrangement is

required to protect the plasmatron (i.e., the plasma generator) from excessive heating. The equipment consists of the following modules [**39**].

- The plasmatron : It is the device which houses the electrodes and in which the plasma reaction takes place. It has the shape of a gun and it is connected to the water cooled power supply cables, powder supply hose and gas supply hose.

- The power supply unit : Normally plasma arc works in a low voltage (40-70 volts) and high current (300-1000 Amperes), DC ambient. The available power (AC, 3 phase, 440 V) must be transformed and rectified to suit the reactor. This is taken care of by the power supply unit.

- The powder feeder : The powder is kept inside a hopper. A separate gas line directs the career gas which fluidizes the powder and carries it to the plasma arc. The flow rate of the powder can be controlled precisely.

- The coolant water supply unit : It circulates water into the plasmatron, the power supply unit, and the power cables. Units capable of supplying refrigerated water are also available.

- The control unit : Important functions (current control, gas flow rate control etc.) are performed by the control unit. It also consists of the relays and solenoid valves and other interlocking arrangements essential for safe running of the equipment. For example the arc can only be started if the coolant supply is on and water pressure and flow rate is adequate.

The Requirements for Plasma Spraying

Roughness of the substrate surface : A rough surface provides a good coating adhesion. A rough surface provides enough room for anchorage of the splats facilitating bonding through mechanical interlocking. A rough surface is generally created by shot blasting technique. The shots are kept inside a hopper, and compressed air is supplied at the bottom of the hopper. The shots are taken afloat by the compressed air stream into a hose and ultimately directed to

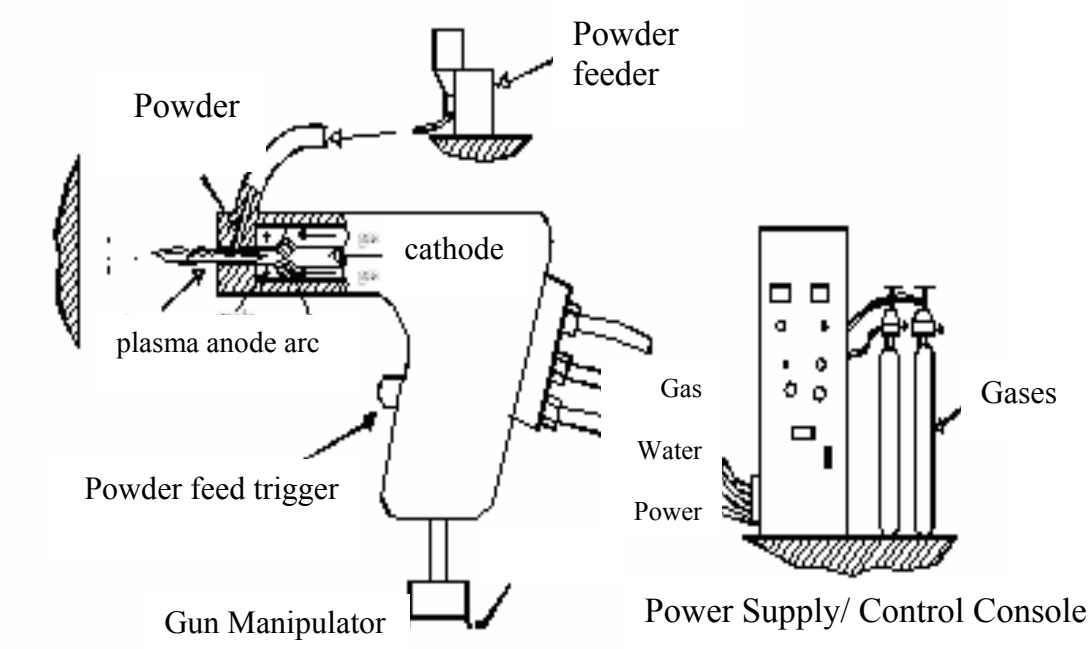

Fig. 2.8 Arrangement for the plasma spraying

an object kept in front of the exit nozzle of the hose. The shots used for this purpose are irregular in shape, highly angular in nature, and made up of hard material like alumina, silicon carbide, etc. Upon impact they create small craters on the surface by localized plastic deformation, and finally yield a very rough and highly worked surface. The roughness obtained is determined by shot blasting parameters, i.e., shot size, shape and material, air pressure, standoff distance between nozzle and the job, angle of impact, substrate material etc. [**40**] . The effect of shot blasting parameters on the adhesion of plasma sprayed alumina has been studied [**37, 38**]. Mild steel serves as the substrate material. The adhesion increases proportionally with surface roughness and the parameters listed above are of importance. A significant time lapse between shot blasting and plasma spraying causes a marked decrease in bond strength [**42**].

Cleanliness of the substrates: The substrate to be sprayed on must be free from any dirt or grease or any other material that might prevent intimate contact of the splat and the substrate. For this purpose the substrate must be thoroughly cleaned (ultrasonically, if possible) with a solvent before spraying. Spraying must be conducted immediately after shot blasting and cleaning. Otherwise on the nascent surfaces, oxide layers tend to grow quickly and moisture may also affect the surface. These factors deteriorate the coating quality drastically [**42**].

Bond coat : Materials like ceramic cannot be sprayed directly onto metals, owing to a large difference between their thermal expansion coefficients. Ceramics have a much lower value of α and hence undergo much less shrinkage as compared to the metallic base to form a surface in compression. If the compressive stress exceeds a certain limit, the coating gets peeled off. To alleviate this problem a suitable material, usually metallic of intermediate a value is plasma sprayed on to the substrate followed by the plasma spraying of ceramics. Bond coat may render itself useful for metallic top coats as well. Molybdenum is a classic example of bond coat for metallic top coats. Molybdenum adheres very well to the steel substrate and develops a somewhat rough top surface ideal for the top coat spraying. The choice of bond coats depends upon the application. For example, in wear application, an alumina and Ni-AI top and bond coats combination can be used [**43**]. In thermal barrier application, CoCrAlY or Ni-AI bond coat [**44**] and zirconia top coat are popular. Ceramic coatings when subjected to hertzian loading deform elastically and the metallic substrate deforms plastically. During unloading, elastic recovery of the coating takes place, whereas for the metallic substrate a permanent set has already taken place. Owing to this elastoplastic mismatch the coating tends to spall off at the interface. A bond coat can reduce this mismatch as well [**45**].

Cooling water : For cooling purpose distilled water should be used, whenever possible. Normally a small volume of distilled water is recirculated into the gun and. it is cooled by an external water supply from a large tank. Sometime water from a large external tank is pumped directly into the gun [**39**] .

Process parameters in plasma spraying

In plasma spraying one has to deal with a lot of process parameters, which determine the degree of particle melting, adhesion strength and deposition efficiency of the powder [**46**]. Deposition efficiency is the ratio of amount of powder deposited to the amount fed to the gun. An elaborate listing of these parameters and their effects are reported in the literature [**47 - 50**].

Some important parameters and their roles are listed below:

Arc power : It is the electrical power drawn by the arc. The power is injected in to the plasma gas, which in turn heats the plasma stream. Part of the power is dissipated as radiation

and also by the gun cooling water. Arc power determines the mass flow rate of a given powder that can be effectively melted by the arc.. Deposition efficiency improves to a certain extent with an increase in arc power, since it is associated with an enhanced particle melting [**42,47,51**]. However, increasing power beyond a certain limit may not cause a significant improvement. On the contrary, once a complete particle melting is achieved, a higher gas temperature may prove to be harmful. In the case of steel, at some point vaporization may take place lowering the deposition efficiency.

Plasma gas: Normally nitrogen or argon doped with about 10% hydrogen or helium is used as a plasma gas. The major constituent of the gas mixture is known as primary gas and the minor is known as the secondary gas. The neutral molecules are subjected to the electron bombardment resulting in their ionization. Both temperature and enthalpy of the gas increase as it absorbs energy. Since nitrogen and hydrogen are diatomic gases, they first undergo dissociation followed by ionization. Thus they need higher energy input to enter the plasma state. This extra energy increases the enthalpy of the plasma. On the other hand, the mono-atomic plasma gases, i.e. argon or helium, approach a much higher temperature in the normal enthalpy range. Good heating ability is expected from them for such high temperature [**52**]. In addition, hydrogen followed by helium has a very high specific heat, and therefore is capable of acquiring very high enthalpy. When argon is doped with helium the spray cone becomes quite narrow which is especially useful for spraying on small targets.

Carrier gas: Normally the primary gas itself is used as a carrier gas. The flow rate of the career gas is an important factor. A very low flow rate cannot convey the powder effectively to the plasma jet, and if the flow rate is very high then the powders might escape the hottest region of the jet. There is an optimum flow rate for each powder at which the fraction of unmelted powder is minimum and hence the deposition efficiency is maximum [**47**].

Mass flow rate of powder : Ideal mass flow rate for each powder has to be determined. Spraying with a lower mass flow rate keeping all other conditions constant results in under utilization and slow coating buildup. On the other hand, a very high mass flow rate may give rise to an incomplete melting resulting in a high amount of porosity in the coating. The unmelted powders may bounce off from the substrate surface as well keeping the deposition efficiency low [**46, 47**].

Torch to base distance : It is the distance between the tip of the gun and the substrate surface. A long distance may result in freezing of the melted particles before they reach the target, whereas a short standoff distance may not provide sufficient time for the particles in flight to melt [**42, 47**]. The relationship between the coating properties and spray parameters in spraying alpha alumina has been studied in details [**53**]. It is found that the porosity increases and the thickness of the coating (hence deposition efficiency) decreases with an increase in standoff distance. The usual alpha-phase to gamma-phase transformation during plasma spraying of alumina has also been restricted by increasing this distance. A larger fraction of the unmelted particles go in the coating owing to an increase in torch to base distance.

Spraying angle: This parameter is varied to accommodate the shape of the substrate. In coating alumina on mild steel substrate, the coating porosity is found to increase as the spraying angle is increased from 30° to 60°. Beyond 60° the porosity level remains unaffected by a further increase in spraying angle [**54**]. The spraying angle also affects the adhesive strength of the coating [**55, 56**]. The influence of spraying angle on the cohesive strength of chromia, zirconia 8-wt% yttria and molybdenum has been investigated, and it has been found that the spraying angle does not have much influence on the cohesive strength of the coatings [**57**].

Substrate cooling: During a continuous spraying, the substrate might get heated up and may develop thermal-stress related distortion accompanied by a coating peel-off. This is especially true in situations where thick deposits are to be applied. To harness the substrate temperature, it is kept cool by an auxiliary air supply system. In addition, the cooling air jet removes the unmelted particles from the coated surface and helps to reduce the porosity [**42**].

Powder related variables: These variables are powder shape, size and size distribution, processing history, phase composition etc. They constitute a set of extremely important parameters. For example, in a given situation if the powder size is too small it might get vaporized. On the other hand a very large particle may not melt substantially and therefore will not deposit. The shape of the powder is also quite important. A spherical powder will not have the same characteristics as the angular ones, and hence both could not be sprayed' using the same set of parameters [**34, 58, 59**].

Preheating of the substrate: The nascent shot blasted surface of the substrate absorbs water and oxygen immediately after shot blasting. Before spraying, the substrate should be preheated to remove moisture from the surface and also for a sputter cleaning effect of the surface by the ions of the plasma [**42**].

Angle of powder injection: Powders can be injected into the plasma jet perpendicularly, coaxially, or obliquely. The residence time of the powders in the plasma jet will vary with the angle of injection for a given carrier gas flow rate. The residence time in turn will influence the degree of melting of a given powder. For example, to melt high melting point materials a long residence time and hence oblique injection may prove to be useful. The angle of injection is found to influence the cohesive and adhesive strength of the coatings as well [**7,39**].

WEAR RESISTANT COATINGS

Today a variety of materials, e.g., carbides, oxides, metallic, etc., belonging to the above category are available commercially. The wear resistant coatings can be classified into the following categories: [**7**]

(i) Carbides: WC, TiC, SiC, ZrC, Cr_2C_3 etc.
(ii) Oxides: Al_2O_3, Cr_2O_3, TiO_2, ZrO2 etc.
(iii) Metallic: NiCrAlY, Ni-Al, Fe-Al, Triballoy etc.
(iv) Diamond

The choice of a material depends on the application. However, the ceramic coatings are very hard and hence on an average offer more abrasion resistance than their metallic counterparts.

Carbide Coatings

Amongst carbides, WC is very popular for wear and corrosion applications [**56**]. The WC powders are clad with a cobalt layer. During spraying the cobalt layer undergoes melting and upon solidification form a metallic matrix in which the hard WC particles remain embedded. Spraying of WC-Co involves a close control of the process parameters such that only the

cobalt phase melts without degrading the WC particles. Such degradation may occur in two ways:

- Oxidation of WC leading to the formation of $CoWO_4$ and WC_2 [**61**].
- Dissolution of WC in the cobalt matrix leading to a formation of brittle phases like CoW_3C which embrittles the coating [**62**].

An increase in the spraying distance and associated increase of time in flight lead to a loss of carbon and a pickup of oxygen. As a result the hardness of the coating decreases [**63**]. An increase in plasma gas flow rate reduces the dwell time and hence can control the oxidation to some extent. However, it increases the possibility of cobalt dissolution in the matrix [**64**]. The other option to improve the quality of such coating is to conduct the spraying procedure in vacuum [**62**].

Often carbides like TiC, TaC and NbC are provided along with WC in the cermet to improve upon the oxidation resistance, hardness, and hot strength. Similarly the binder phase is also modified by adding chromium and nickel with cobalt [**7**]. The wear mechanism of plasma sprayed WC-Co coatings depends on a number of factors, e.g., mechanical properties, cobalt content, experimental conditions, mating surfaces, etc. The wear mode can be abrasive, [**65, 66, 67**] adhesive or surface fatigue [**68, 69**]. The coefficient of friction of WC-Co (in self mated condition) increases with increasing cobalt content [**68**]. A WC-Co coating when tested at a temperature of 450°C exhibits signs of melting [**70**]. The wear resistance of these coatings also depends on porosity [**66**]. Pores can also act as source from where the cracks may grow. Thermal diffusivity of the coatings is another important factor. In narrow contact regions, an excessive heat generation may occur owing to rubbing. If the thermal diffusivity of the coating is low the heat cannot escape from a narrow region easily resulting a rise in temperature and thus failure occurs owing to thermal stress [**66, 70**]. The wear mechanism of WC-Co nanocomposite coating on mild steel substrates has been studied in details [**71**]. The wear rates of such coatings are found to be much greater than that of commercial WC-Co composite coating, presumably owing to an enhanced decomposition of nanoparticles during spraying. Wear has been found to occur by subsurface cracking along the preferred crack paths provided by the binder phase or failure at the inter-splat boundary.

Coatings of TiC or TiC+ TaC with a nickel cladding are alternative solutions for wear and corrosion problems. High temperature stability, low coefficient of thermal expansion, high

hardness and low specific gravity of these coatings may outperform other materials, especially in steam environment [**7**]. Instead of nickel, nickel chromium alloy can serve as the matrix material [**72, 73**]. The mode of wear can be adhesive, abrasive, surface fatigue or micro-fracture depending on operating conditions [**69, 73**].

A coating of Cr_3C_2 (with Ni-Cr alloy cladding) is known for its excellent sliding wear resistance and superior oxidation and erosion resistance, though its hardness is lower than that of WC [**7**]. After spraying in air, Cr_3C_2 loses carbon and transforms to Cr_7C_3. Such transformation generally improves hardness and erosion resistance of the coating [**74**]. The sliding wear behaviour of the Cr_3C_2 -Ni -Cr composite has been studied by several authors against various metals and ceramics [**66, 69, 75**]. It is felt that at lower loads the wear is owing to the detachment of splats from the surface. As the load increases, melting, plastic deformation and shear failure come into play.

Oxide Coatings

Metallic coatings and metal containing carbide coatings sometime are not suitable in high temperature environments in both wear and corrosion applications. Often they fail owing to oxidation or decarburization. In such case the material of choice can be an oxide ceramic coating, e.g., $Al_2O_3.Cr_2O_3$, TiO_2, ZrO_2 or their combinations. However, a high wear resistance, and chemical and thermal stability of these materials are counterbalanced by the disadvantages of low values of thermal expansion coefficient, thermal conductivity, mechanical strength, fracture toughness and somewhat weaker adhesion to substrate material. The thickness of these coatings is also limited by the residual stress that grows with thickness. Therefore, to obtain a good quality coating it is essential to exercise proper choice of bond coat, spray parameters and reinforcing additives [**7**].

Chromia (Cr_2O_3) Coatings

These coatings are applied when corrosion resistance is required in addition to abrasion resistance. It adheres well to the substrate and shows an exceptionally high hardness 2300 $HV_{0.5\,kg}$ [**7**]. Chromia coatings are also useful in ship and other diesel engines, water pumps, and printing rolls [**7**]. A Cr_2O_3- 40 wt% TiO_2 coating provides a very high coefficient of friction (0.8), and hence can be used as a brake liner [**7**]. The wear mode of chromia coatings

has been investigated under various conditions. Depending on experimental conditions, the wear mode can be abrasive [**68**], plastic deformation [**69, 70, 76**], microfracture [**77**] or a conglomerate of all of these [**78**]. This material has also been tested under lubricated conditions, using inorganic salt solutions (NaCl, $NaNO_3$, Na_3PO_4) as lubricants and also at a high temperature. The wear rate of self-mated chromia is found to increase considerably at 450°C, and plastic deformation and surface fatigue are the predominant wear mechanisms [**79**]. Under lubricated condition, the coatings exhibit tribochemical wear [**80**]. It has also been tested for erosion resistance [**81**].

Zirconia (ZrO_2) Coatings

Zirconia is widely used as a thermal barrier coating. However, it is endowed with the essential qualities of a wear resistant material, i.e., hardness, chemical inertness, etc. and shows reasonably good wear behaviour. In the case of a hot pressed zirconia mated with high chromium containing iron (martensitic, austenitic, or pearlitic), it has been found that in course of rubbing the iron transfers on to the ceramic surface and the austenitic material adheres well to the ceramic as compared to their martensitic or pearlitic counterparts [**82**]. The thick film improves the heat transfer from the contact area keeping the contact temperature reasonably low; thus the transformation of ZrO_2 is prevented. On the other hand with the pearlitic or martensitic iron the material transfer is limited. The contact temperature is high enough to bring about a phase transformation and related volume change in ZrO_2 causing a stress induced spalling. In a similar experiment the wear behaviour of sintered, partially stabilized zirconia (PSZ) with 8 wt% yttria against PSZ and steels has been tested at 200°C. When metals are used as the mating surface, a transferred layer soon forms on the ceramic surface (coated or sintered) [**83**]. In ceramic-ceramic system the contact wear is abrasive in nature. However, similar worn particles remain entrapped between the contact surfaces and induce a polishing wear too. In the load range of 10 to 40 N, no transformation of ZrO_2 occurs [**83, 84**]. However, similar tests conducted at 800°C show a phase transformation from monoclinic ZrO_2 to tetragonal ZrO_2 [**85**]. The wear debris of ZrO_2 sometimes get compacted in repeated loading and gets attached to the worn surface forming a protective layer [**86**]. During rubbing, pre-existing or newly formed cracks may grow rapidly and eventually interconnect with each other, leading to a spalling of the coating [**87**]. The worn particles get entrapped between the mating surfaces and abrade the coating. The wear performance of ZrO_2-12 mol% CeO_2 and ZrO_2-12 mol% CeO_2 -10 mol% Al_2O_3

coatings against a bearing steel under various loads has been studied [**88**]. Introduction of alumina as a dopant, has been found to improve the wear performance of the ceramic significantly. Here plastic deformation is the main wear mode. The wear performance of zirconia at 400°C and 600°C has been reported in the literature [**89**]. At these temperatures the adhesive mode of wear plays the major role.

Titania (TiO_2) Coating

Titania coating is known for its high hardness, density, and adhesion strength [**66, 69**]. It has been used to combat abrasive, erosive and fretting wear either in essentially pure form or in association with other compounds [**90, 91**]. The mechanism of wear of TiO_2 at 450°C under both lubricated and dry contact conditions has been studied [**69, 70**]. It has been found to undergo a plastic smearing under lubricated contact, where as it fails owing to the surface fatigue in dry condition. TiO_2-stainless steel couples in various speed load conditions have also been investigated in details [**92**]. At a relatively low load, the failure is owing to the surface fatigue and adhesive wear, whereas at a high load the failure is attributed to the abrasion and delamination associated with a back and forth movement [**93**]. At low speed the transferred layer of steel oxidizes to form Fe_2O_3 and the wear progresses by the adhesion and surface fatigue. At a high speed, Fe_3O_4 forms instead of Fe_2O_3 [**94**]. The TiO_2 top layer also softens and melts owing to a steep rise in temperature, which helps in reducing the temperature subsequently [**95**]. The performance of the plasma sprayed pure TiO_2 has been compared with those of Al_2O_3 – 40 wt% TiO_2 and pure Al_2O_3 under both dry and lubricated contact conditions [**96**]. TiO_2 shows the best results. TiO_2 owing to its relatively high porosity can provide good anchorage to the transferred film and also can hold the lubricants effectively [**97**].

Alumina (Al_2O_3) Coatings

Alumina is obtained from a mineral called bauxite, which exists in nature as a number of hydrated phases, e.g., boehmite (γ-Al_2O_3, H_2O), hydragillate, diaspore (α-Al_2O_3. $3H_2O$). It also exists in several other metastable forms like β, δ, θ, η, κ and X [**98**]. α -Al_2O_3 is known to be a stable phase and it is available in nature in the form of corundum. In addition, α-Al_2O_3 can be extracted from the raw materials by fusing them.

The phase transformation during freezing of the plasma sprayed alumina droplets has been studied in details [**99, 100**]. From the molten particles, γ-Al_2O_3 tends to nucleate, since liquid to γ transformation involves a low interfacial energy. The phase finally formed upon cooling depends on the particle diameter. For particle diameter less than 10 μm, the metastable form is retained (γ, δ, β or θ). Plasma spraying of alumina particles having a mean diameter of 9 μm results in the development of the gamma phase in the coating after cooling [**101**]. The α form is found in the large diameter particle. In fact larger is the diameter; greater is the fraction of α-Al_2O_3 in the cooled solid. This form is desirable for its superior wear properties. Other than the cooling rate, one way to achieve the phase finally formed is to vary the temperature of the substrate. If the substrate temperature is kept at 900^0C, the δ phase forms. The α-Al_2O_3 can be formed by raising the temperature of the substrate to 1100^0 C resulting a slow cooling. During freezing the latent heat of solidification is absorbed in the still molten pool. If this heat generation is balanced by the heat transfer to the substrate, columnar crystals grow. On the other hand, if the aforesaid heat transfer is faster than the heat injection rate from the growing solidification front, equi-axed crystals are supposed to form. In reality columnar crystals are generally found.

There are several advantages of alumina as a structural material, e.g., availability, hardness, high melting point, resistance to wear and tear etc. It bonds well with the metallic substrates when applied as a coating on them. Some of the applications of alumina are in bearings, valves, pump seals, plungers, engine components, rocket nozzles, shields for guided missiles, vacuum tube envelops, integrated circuits, etc. Plasma sprayed alumina-coated railroad components are presently being used in Japan [**102**].

Properties of alumina can be further complemented by the particulate (TiO_2, TiC) or whisker (SiC) reinforcement [**103**]. TiC reinforcement limits the grain growth, improves strength and hardness, and also retards crack propagation through the alumina matrix [**104**]. The sliding wear behaviour of both monolithic and SiC whisker reinforced alumina has been studied [**105**]. The whisker reinforced composite has been found to have good wear resistance. The monolithic alumina has a brittle response to sliding wear, whereas the worn surface of the composite reveals signs of plastic deformation along with fracture. The whiskers also undergo pullout or fracture.

TiO_2 is a commonly used additive in plasma sprayable alumina powder [**106, 107**]. TiO_2 has a relatively low melting point and it effectively binds the alumina grains. However, a success of an Al_2O_3 - TiO_2 coating depends upon a judicious selection of the arc current, which can melt the powders effectively. This results in a good coating adhesion along with high wear resistance [**51**]. The wear performance of Al_2O_3 and Al_2O_3 -50 wt% TiO_2 has been reported in the literature [**96**]. In dry sand abrasion testing, alumina outperformed others presumably owing to its high hardness [**108**]. In dry sliding at low velocity range, the tribocouple (ceramic and hardened stainless steel) exhibits stick-slip [**109**]. At relatively high speed range, the coefficient of friction drops owing to the thermal softening of the interface [**95**]. The wear of alumina is found to increase appreciably beyond a critical speed and a critical load. Alumina has been found to fail by plastic deformation, shear and grain pullout. In dry and lubricated sliding as well, the mixed ceramic has been found to perform better than pure alumina. A coating of Al_2O_3 -50 wt% TiO_2 is quite porous and hence is quite capable of holding the transferred metallic layer which protects the surface [**97**]. Wear performance of such coatings can further be improved by a sealing of the pores by polymeric substances [**43**]. A low thermal diffusivity of the alumina coatings results in a high localized thermal stress on the surface. The mode of wear of alumina is mainly abrasive. The pore size and pore size distribution also play a vital role in determining the wear properties. The Al_2O_3 - TiO_2 coating has a high thermal diffusivity and hence it is less prone to wear.

The sliding wear behaviour of plasma sprayed alumina against AISI-D2 steel under different speed load conditions has been reported [**110**]. Within the load range used (45N-133N), the wear vs load plot shows a maxima. In the initial phase, the wear volume increases with the load for a given number of sliding cycles. Beyond a certain load, owing to both load and frictional heating, a major plastic flow occurs on the coating surface. The plastic flow leads to an increase in real area of contact and a corresponding reduction of normal stress, though the normal load increases [**111**]. As a result, wear decreases with an increase in load beyond a critical normal load. On the other hand, the wear vs. sliding speed plot also displays a maxima within the speed range used (0.31 to 8 m/s). At a low speed range, the asperities move against each other and deform each other in the process. As the speed is increased, the asperities are subjected to heavy impacts and tend to get fractured from the root producing a higher volume of debris. At a very high velocity the friction related temperature rise becomes high enough to soften the asperities and thereby to protect them from fracture. The wear rate

keeps low under such circumstances. Therefore, the plastic deformation and brittle fracture form the failure mechanisms.

Metallic Coatings

Metallic coatings can be easily applied by flame spraying or welding techniques making the process very economical. Moreover plasma sprayable metallic consumables are also available in abundant quantity. Metallic wear resistant materials are classified into three categories:

(i) cobalt based alloys
(ii) nickel based alloys
(iii) iron based alloys

The common alloying elements in a cobalt-based alloy are Cr, Mo, W and Si. The microstructure is constituted by dispersed carbides of M_7C_3 type in a cobalt rich FCC matrix. The carbides provide the necessary abrasion resistance and corrosion resistance. Hardness at elevated temperatures is retained by the matrix [**112, 113**]. Sometimes a closed packed inter-metallic compound is formed in the matrix, which is known as the Laves phase. This phase is relatively soft but offers significant wear resistance [**114**]. The principal alloying elements in Ni-based alloys are Si, B, C and Cr. The abrasion resistance can be attributed to the formation of extremely hard chromium borides. Besides carbides, Laves phase is also present in the matrix [**112**].

Iron based alloys are classified into pearlitic steels, austenitic steels, martensitic steels and high alloy irons. The principal alloying elements used are Mo, Ni, Cr and C. The softer materials, e.g., ferritic, are for rebuilding purpose. The harder materials, e.g., martensitic, on the other hand provide wear resistance. Such alloys do not posses much corrosion, oxidation or creep resistance [**112, 115, 116**]. NiCoCrAlY is an example of plasma sprayable superalloy. It shows an excellent high temperature corrosion resistance and hence finds application in gas turbine blades. The compositional flexibility of such coatings permits tailoring of such coating composition for both property improvement and coating substrate compatibility. In addition, it serves as a bond coat for zirconia based thermal barrier coatings [**7, 117**].

Diamond Coatings

Thin diamond films for industrial applications are commonly produced by CVD, plasma assisted CVD, ion beam deposition, and laser ablation technique [**118, 119**]. Such coatings are used in electronic devices and ultra wear resistant overlays. The limitation of the aforesaid methods is their slow deposition rates. The DIA-JET process involving a DC Ar/H2 plasma with methane gas supplied at the plasma jet is capable of depositing diamond films at a high rate [**120**]. However, the process is extremely sensitive to the process parameters. Deposition of diamond film is also possible using a oxy-acetylene torch [**121**]. One significant limitation of a diamond coating is that it cannot be rubbed against ferrous materials, owing to a phase transformation leading to the formation of other carbon allotropes [**122**]. Diamond films are tested for the sliding wear against abrasive papers, where wear progresses by micro fracturing of protruding diamond grits. The process continues till the surface becomes flat and thereafter wear progresses by an interfacial spalling. Therefore, the life of the coating is limited by its thickness [**123**].

Nickel Aluminide Coatings

Nickel aluminide is another example of a potential coating material. The mixture of Ni-Al powders, when sprayed, reacts exothermically to form nickel aluminide. This reaction improves the coating substrate adhesion. In addition to wear related application, it is mostly used as bond coat for ceramic materials [**44**]. Nickel based coatings are used in applications when wear resistance combined with oxidation or hot corrosion resistance is required [**124**]. In fact, nickel based alloys represent a significant part of overall thermal spray business. These materials are widely used as bond coats in number of applications requiring combination of properties, such as good wear resistance and corrosion resistance at the same time [**125,126**]. Inter-metallic compounds also find extensive use in high temperature structural applications [**3,4,127,128**]. In particular, nickel-aluminium alloys and their derivatives have potential demand in aerospace industry and other high performance applications as the yield strength of these alloys increases with increasing temperature up to 600^{o} C [**3, 4**].

Nickel aluminide, Ni_3Al, has drawn enormous attention because of its technological and scientific interest. Technologically Ni_3Al is the most important strengthening constituent,

used extensively as high temperature structural materials for jet engine and aerospace applications. It is responsible for the strength and creep resistance of the super alloys at elevated temperatures Ni_3Al containing about 25 wt % Al has the ability to form protective aluminum oxide scales, resulting in excellent oxidation resistance. Industrial interest in Ni_3Al based alloys is high at the present time. This interest arises because the alloys possess a unique combination of properties including high strength and good oxidation and corrosion resistance at elevated temperatures and relatively low density compared with many Nickel-base, high temperatures super alloys. A brief summary of these applications are given in table 2.1. [**129**].

PROPERTIES	APPLICATIONS
• Improved fatigue life and potential for low cost	• Turbo Charger rotors in diesel engine trucks.
• Good high temperature oxidation resistance, excellent strength at high strain rates.	• Die materials for isothermal forging. Mold material for glass processing
• Resistance to carburizing and oxidizing atmospheres.	• Fixture material for heat treatment of auto parts in high temperature furnaces.
• High temperature strength, good oxidation & corrosion resistance.	• Rollers for steel slab heating furnaces.
• Excellent vibration, cavitations resistance in water	• Hydro turbine rotors
• Low & high temperature strength & cutting properties.	• Cutting tools.
• Superior strength & creep resistance.	• Turbine blades vanes for jet engines.

Table 2.1 Properties and Applications of Nickel-Aluminide

EROSION WEAR OF SURFACE COATINGS

Solid Particle Erosion (SPE) is a wear process where particles strike against surfaces and promote material loss. During flight a particle carries momentum and kinetic energy, which can be dissipated during impact, due to its interaction with a target surface. Different models have been proposed that allow estimations of the stresses that a moving particle will impose on a target [**130**]. It has been experimentally observed by many investigators that during the impact the target can be locally scratched , extruded , melted and/or cracked in different ways [**131,132,133**] . The imposed surface damage will vary with the target material, erodent

particle, impact angle, erosion time, particle velocity, temperature and atmosphere [**131,134**] .

Plasma sprayed coatings are used today as erosion or abrasion resistant coatings in a wide variety of applications [**135**] . Extensive research shows that the deposition parameters like energy input in the plasma and powder properties affect the porosity, splat size, phase composition, hardness etc. of plasma sprayed coatings [**136 - 140**]. These in turn, have an influence on the erosion wear resistance of the coatings. Quantitative studies of the combined erosive effect of repeated impacts are very useful in predicting component lifetimes, in comparing the performance of materials and also in understanding the underlying damage mechanisms involved.

Resistance of engineering components encountering the attack of erosive environments during operation can be improved by applying ceramic coatings on their surfaces. Alonso et. al. [**141**] experimented with the production of plasma sprayed erosion-resistant coatings on carbon-fiber-epoxy composites and the studied of their erosion behaviour. The heat sensitivity of the composite substrate requires a specific spraying procedure in order to avoid its degradation. In addition, several bonding layers were tried to allow spraying of the protective coatings. Two different functional coatings; a cermet (WC-12 Co) and a ceramic oxide (Al_2O_3) were sprayed onto an aluminium-glass bonding layer. The microstructure and properties of these coatings were studied and their erosion behaviour determined experimentally in an erosion-testing device. Tabakoff and Shanov [**142**] designed a high temperature erosion test facility to provide erosion data in the range of operating temperatures experienced in compressors and turbines. In addition to the high temperatures, the facility properly simulates all the erosion parameters important from the aerodynamics point of view. These include particle velocity, angle of impact, particle size, particle concentration and sample size. They reported the erosion behavior of titanium carbide coating exposed to fly ash and chromite particles. Chemical vapor deposition technique (CVD) was used to apply a ceramic coating on nickel and cobalt based super-alloys (M246 and X40). The test specimens were exposed to particle-laden flow at velocities of 305 and $366ms^{-1}$ and temperatures of 550°C and 815°C.

Number of reports are available on erosion behaviour of alumina coatings. The resistance to erosion of such coatings depends upon inter-splat cohesion, shape, size, and hardness of

erodent particles, particle velocity, angle of impact and the presence of cracks and pores [**143 -147**]. The slurry (SiC and SiO_2) and airborne particle (Al_2O_3 and SiO_2) erosions of flame sprayed alumina coatings have also been reported in the literature [**95**]. SiC and Al_2O_3 are found to cause significant amount of erosion in slurry and airborne erosion testing respectively. High particle velocity enhances the erosion rate and the erosion rate is maximum for an impact angle of 90^0. The failure is by the progressive removal of splats and can be attributed to the presence of defects and pores in the inter-splat regions. Similar observation has been made for the plasma sprayed alumina coatings subjected to an erosive wear caused by the SiO_2 particles [**148**]. Branco *et. al*. [**149**] examined room temperature solid particle erosion of zirconia and alumina-based ceramic coatings, with different levels of porosity and varying microstructure and mechanical properties. The erosion tests were carried out by a stream of alumina particles with an average size of 50 μm at 70m/s, carried by an air jet with impingement angle of 90^0. The results indicate that there is a strong relationship between the erosion rate and the coating porosity.

It is evident from the literature review that nickel-aluminide has long been used as a coating material on industrial and structural elements. But its role has mostly been restricted as a bond coat between the core component and the ceramic top coat. Its use as a top coat material has not been reported so far. A recent paper by Mishra et. al. [**150**] reports the erosion behaviour of plasma sprayed Ni_3Al coating on a Fe-based super-alloy where the erosion rate of the coating is found to be marginally higher than the superalloy regardless the impact angle. In this study, nickel-aluminide is coated on the top surface but there is a plasma sprayed NiCrAlY bond coat also between the substrate and the Ni_3Al top coat.

Against this background, the present research work is undertaken to deposit nickel-aluminide coatings on metallic substrate without any intermediate bond coat and to explore its potential as a functional top coat material. Mild steel and copper are chosen as the substrate material and the deposition of Ni-Al is made by atmospheric plasma spray coating route.

OBJECTIVE

The objective of the present investigation can be stated as following:

a. Development of plasma sprayed nickel-aluminide top coat on metallic substrates.
b. Micro-structural characterization to evaluate the soundness of the coatings.

c. Mechanical characterization to evaluate the micro-hardness and interface bond strength of the coatings.
d. Assessment of the capabilities of the coatings to combat wear with a special reference solid particle erosion wear.
e. Complementing the experimental results, in regard to coating deposition efficiency and wear behaviour by predicted results obtained from an artificial neural network analysis.

******

Chapter 3

EXPERIMENTAL METHODS

CHAPTER 3

MATERIALS AND METHODS

INTRODUCTION

This chapter deals with the details of the experimental procedures followed in this work. The coating procedure itself requires some basic preparation, i.e., grit blasting and cleaning. After plasma spraying, the coated materials are subjected to a series of tests, e.g., micro-structural characterization of the surfaces and cross sections, porosity and micro-hardness measurement, X - ray diffraction studies, adhesion test, erosion test etc. The details of each of these processes are described here.

PROCESSING OF THE COATINGS

Preparation of Substrates and Coating Materials

Commercially available mild steel (MS) and copper (Cu) were chosen as the substrate materials for the present work. The specimens are rectangular in shape having a dimension 50 mm x 25 mm x 2 mm. The specimens were grit blasted at a pressure of 3 kg/cm^2 using alumina grits having a grit size of 60. The standoff distance in shot blasting was kept between 120-150 mm. The average roughness of the substrates is 6.8 μm. The grit blasted specimens were cleaned with acetone. Spraying is carried out immediately after cleaning.

Nickel and aluminium metal powders of commercial grades are used to produce nickel aluminide coating, which is formed at high temperature during plasma spraying. These two powders Ni : Al were thoroughly mixed in ratio 3:1 by weight. The particle size range the powders used in the study, are given in the table.3.1.

Powder	Range
Aluminum	-106μm to +53μm
Nickel	-74 Aμm to +53 μm

Table 3.1 Particle size range used for coating

The raw powders were characterized for their chemical purity by standard wet chemical analysis. They were found to contain only about 0.8% of the respective metal oxides and were thus more than 99% pure.

PLASMA SPRAYING

The spraying is done using a 40 kW APS (atmospheric plasma spray) system in the thermal plasma laboratory at NIT Rourkela. Conventional atmospheric plasma spraying (APS) set up is used. The plasma input power is varied from 10 to 24 kW by controlling the gas flow rate, voltage and the arc current. The powder feed rate is kept constant at 50 gm/min, using a turntable type volumetric powder feeder.

The general arrangement of the plasma spraying equipment and schematic diagram of the plasma spraying process are shown in figures 3.1 and 3.2 respectively. The equipment consists of the following units:

1. Plasma spraying gun
2. Control console
3. Powder feeder
4. Power supply
5. Torch cooling system (water)
6. Hoses, cables, gas cylinders and accessories

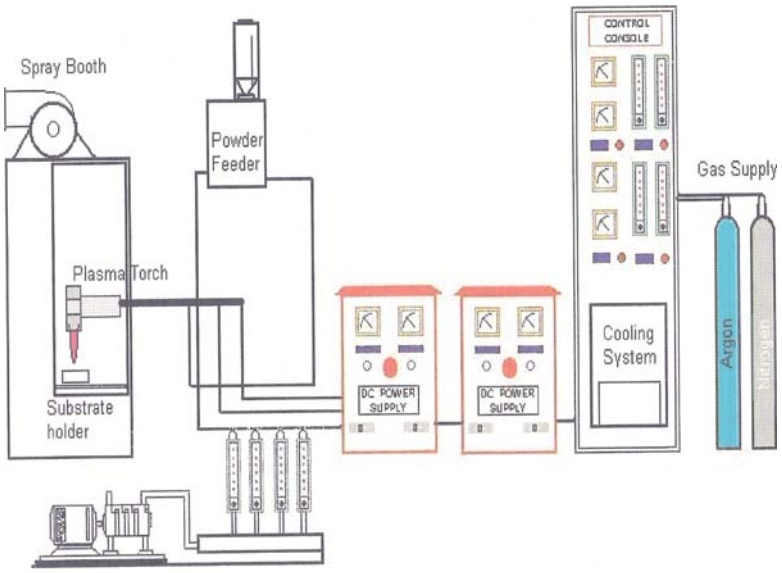

Fig. 3.1 General arrangement of the plasma spraying equipment

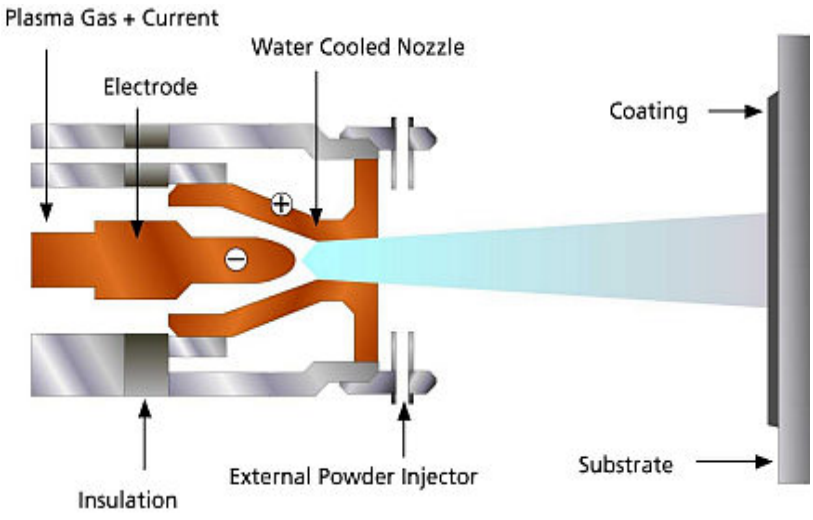

Fig. 3.2 Schematic diagram of the plasma spraying process

Argon is used as the primary plasmagen gas and nitrogen as the secondary gas. The powders are deposited at spraying angle of 90°. The powder feeding is external to the gun. The properties of the coatings are dependent on the spray process parameters. The operating parameters during coating deposition process are listed in table 3.2.

Parameter	Range
Torch input power	10-24 kW
Current	250-480Amp
Voltage	40-50 Volt
Plasma gas (Ar) flow rate	20 lpm
Powder feed rate	50 gm/min
Carrier gas (Ar) flow rate	12 lpm
Torch to base distance	100 mm

Table 3.2 Operating parameters during coating deposition

X-Ray Diffraction Studies

The coatings are examined for the identification of the (crystalline) phases with a Philips X Ray Diffractometer. The X ray diffractograms are taken using Cu Kα radiation. All coated samples have been studied.

Scanning Electron Microscopic Studies

Specimens of size 10 mm x 13 mm x 5 mm are sliced from the coated samples for SEM observation. Both top surface and cross section of specimens are observed in scanning electron microscope **Jeol JSM-6480LV** mostly using the secondary electron imaging. Coating cross-sections are polished in three stages using SiC abrasive papers of reducing grit sizes and then with diamond pastes on a wheel for coating interface analysis under SEM. These specimens are also utilized for the microhardness measurement.

Porosity Measurement

Measurement of porosity is done using the image analysis technique. The polished top coats are kept under a microscope (Neomate) equipped with a CCD camera (JVC, TK 870E). This system is used to obtain a digitized image of the object. The digitized image is transmitted to a computer equipped with VOIS image analysis software. The total area captured by the

objective of the microscope or a fraction thereof can be accurately measured by the software. Hence the total area and the area covered by the pores are separately measured and the porosity of the surface under examination is determined.

Microhardness Measurement

Microhardness measurement is made using Leitz Microhardness Tester equipped with a monitor and a microprocessor based controller, with a load of 0.245N and a loading time of 20 seconds. About ten or more readings are taken on each sample and the average value is reported as the data point.

Evaluation of Coating Deposition Efficiency

Deposition efficiency is defined as the ratio of the weight of coating deposited on the substrate to the weight of the expended feedstock. Weighing method is accepted widely to measure this. Each specimen is weighed before and after coating deposition. The difference is the weight (Gc) of coating deposited on the substrate . From the powder feed rate and time of deposition the weight of expended feed stock (Gp) is determined. The deposition efficiency (η) is then calculated using the following equation [**151**].

$\eta = (G_c / G_p \text{ X } 100) \%$

Weighing of samples is done using a precision electronic balance with $\pm$ 0.1 mg accuracy.

Evaluation of Coating Interface Bond Strength

To evaluate the coating adhesion strength, a special type jig (fig. 3.3) is fabricated. Cylindrical mild steel dummy samples (length 50 mm, top and bottom diameter 12 mm) are prepared. The surfaces of the dummies are roughened by punching. These dummies are then fixed on top of the coating with the help of a polymeric adhesive (epoxy 900-C) and pulled with tension after being mounted on the jig (fig. 3.4). The coating pullout test is carried out using the set up Instron 1195 at a crosshead speed of 10 m/minute.The moment coating gets torn off from the specimen, the reading (of the load), which corresponds to the adhesive strength of the coating, is recorded. A typical test set up (during testing) is shown in figure 3.5. The test is performed as per ASTM C-633.

Fig. 3.3 Jig used for the test

Fig. 3.4 Specimen under tension

Fig. 3.5 Adhesion test set up **Instron 1195**

EROSION WEAR BEHAVIOUR OF COATINGS

Solid particle erosion (SPE) is usually simulated in laboratory by one of two methods. The 'sand blast' method, where particles are carried in an air flow and impacted onto a stationary target and the 'whirling arm' method , where the target is spun through a chamber of falling particles.

In the present investigation, an erosion apparatus (self-made) of the 'sand blast' type is used. It is capable of creating highly reproducible erosive situations over a wide range of particle sizes, velocities, particles fluxes and incidence angles, in order to generate quantitative data on materials and to study the mechanisms of damage. The test is conducted as per ASTM G76 standards.

The jet erosion test rig used in this work employs a 300 mm long nozzle of 3 mm bore and 300 mm long. This nozzle size permits a wider range of particle types to be used in the course of testing, allowing better simulations of real erosion conditions. The mass flow rate is measured by conventional method. Particles are fed from a simple hopper under gravity into the groove. Velocity of impact is measured using double disc method [**152]**. Some of the features of this test set up are:

- Vertical traverse for the nozzle: provides variable nozzle to target standoff distance, which influences the size of the eroded area
- Different nozzles may be accommodated: provides ability to change the particle plume dimensions and the velocity range
- Large test chamber with sample mount (typical sample size 25 mm x 25 mm) that can be angled to the flow direction: by tilting the sample stage, the angle of impact of the particles can be changed in the range of $0^0 - 90^0$ and this will influence the erosion process.

In this work, room temperature solid particle erosion test on mild steel substrates coated with different feed materials is carried out under different impact angles 15^o,30°, 45^o,60° and 90° . The nozzle is kept at 100 and 150 mm stand-off distance from the target. 400 μm average size dry silica sand particles are used as erodent with three different velocities of 31.2 m/s, 44.2 m/s and 58.5 m/s. 6.25 cm^2 area of each coating sample is exposed to the compressed air jet carrying erodent. Amount of wear is determined on 'mass loss' basis. It is done by measuring the mass of the samples at the beginning of the test and at regular intervals in the test duration. A precision electronic balance with $\pm$ 0.1 mg accuracy is used for weighing. Erosion rate, defined as the coating mass loss per unit erodent mass (mg/g) is calculated.

*****

Chapter 4

COATING CHARACTERIZATION: RESULTS & DISCUSSION

CHAPTER 4

COATING CHARACTERIZATION: RESULTS AND DISCUSSION

INTRODUCTION

Coatings of nickel-aluminide were developed on two different substrates (copper and mild steel) using a 40 kW atmospheric plasma spray system. Spray deposition was done at different input power level to the dc plasma torch (in the range 10 kW to 24 kW). Characterization of the coatings was carried out with respect to their quality performance. The results of various characterization studies are presented and discussed in this chapter.

COATING ADHESION STRENGTH

From the microscopic point of view, adhesion is due to physico-chemical surface forces (Vander-walls, Covalent, ionic…etc.), which can be established at the coating-substrate interface [**153**] and corresponds to the work of adhesion. From the mechanical point of view, adherence can be estimated by the force corresponding to interfacial fracture and is macroscopic in nature. Coating adherence tests have been carried out by many investigators with various coatings. It has been stated that the fracture mode is adhesive if it takes place at the coating-substrate interface and that the measured adhesion value is the value of practical adhesion, which later is strictly an interface property, depending exclusively on the surface characteristics of the adhering phase and the substrate surface condition [**154, 155**]

In this work, evaluation of coating interface bond strengths is done using coating pullout method, conforming to ASTM C-633 standard. It is found that, in all the samples fracture occurred at the coating-substrate interface. The adhesion strength of these coatings deposited at different operating power level of the plasma torch on mild steel and copper substrates are presented in table 4.1. Maximum adhesion strength of ≈ 12.5 MPa is recorded on mild steel substrate, for the coating deposited at 20 kW power level.

Substrate	Operating Power Level (kW)	Coating AdhesionStrength (Mpa)
Mild steel	10	7.45
	12	7.98
	16	9.96
	20	**12.50** (Max)
	24	10.27
Copper	10	7.89
	12	8.20
	16	8.65
	20	10.15
	24	6.21

Table 4.1 Coating Adhesion Strength Test Results

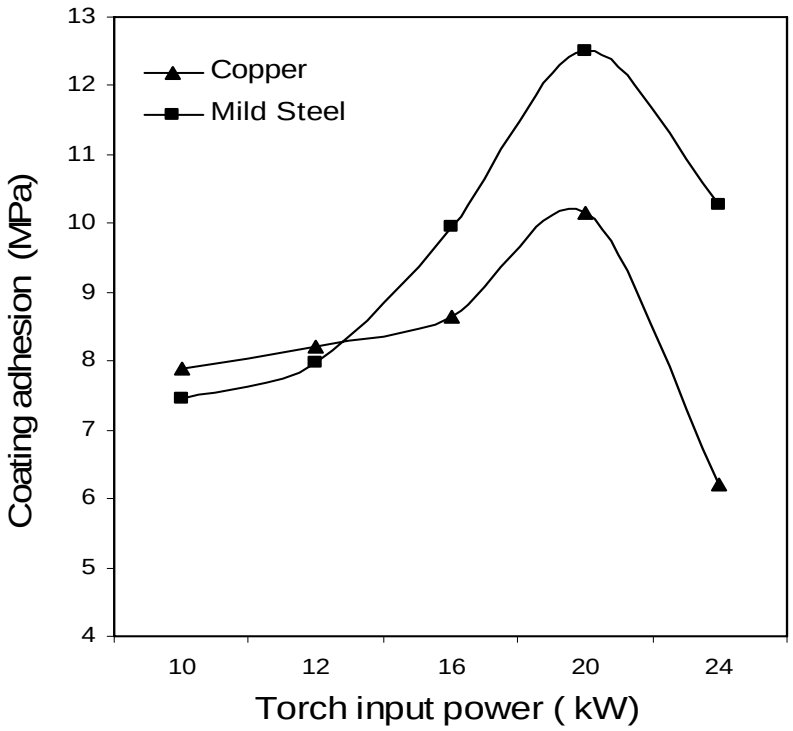

Fig 4.1 Adhesion Strength of nickel-aluminide coatings made at different power level on different substrates

COATING HARDNESS

Micro-hardness measurement was done on the optically distinguishable phases on the coating cross-section (on the interface as well as on the substrate), with a Leitz Micro-hardness Tester using 25 Pa (0.245 N) load on polished cross section of the samples.

Power level (kW)	Testing points	Micro Hardness (HV)
10	On the substrate	163.63
	Interface	680.91
	Intermediate	813.74
	Periphery	189.74
12	On the substrate	143.92
	Interface	299.83
	Intermediate	188.89
	Periphery	151.46
16	On the substrate	125.38
	Interface	364.90
	Intermediate	**917.95**
	Periphery	413.03
20	Interface	181.05
	Intermediate	238.51
	Periphery	160.49

Table 4.2 Coating micro hardness at different operating power levels

The results are summarized in Table 4.2. In Ni-Al coatings four different range of hardness values are observed; ranging from 160 HV to 917 HV. The variation of hardness values may be due to the formation of different phases i.e. aluminides during coating deposition and existence of different alumina phases i.e. α- and γ-alumina etc.

XRD PHASE COMPOSITION ANALYSIS

Micro-hardness test shows different hardness values on different optically distinct regions on the phases of the coating (cross-sections). Therefore, to ascertain the phases present (and if! phase changes / transformation taking place during plasma spraying), the X-ray diffractograms are taken on the raw material and on some selected coatings using a Philips X Ray Diffractometer. The XRD results are shown in figures 4.2 to 4.4.

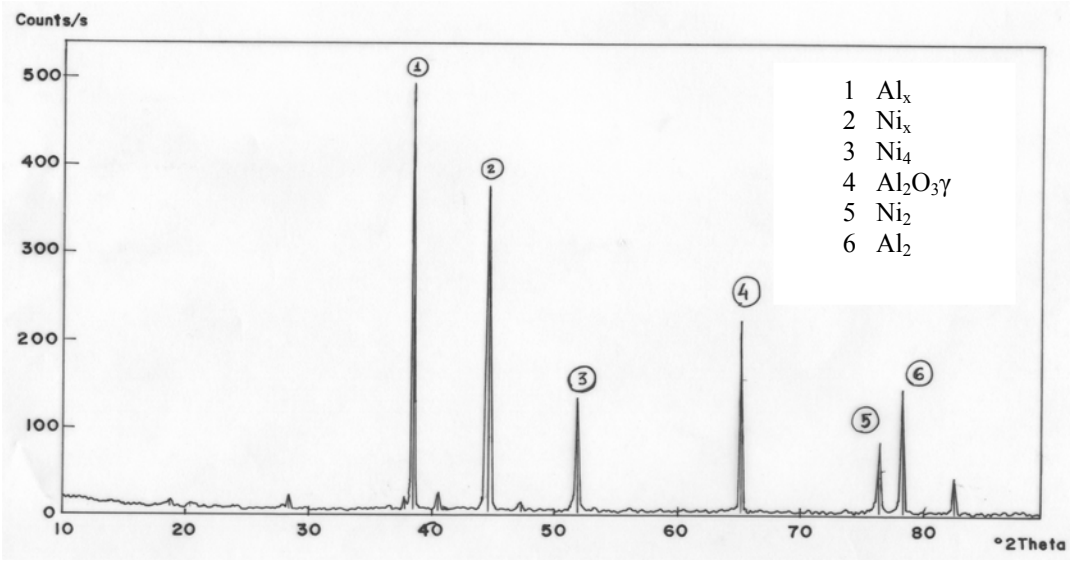

Fig 4.2 X Ray Diffractogram of Nickel-Aluminium raw powder

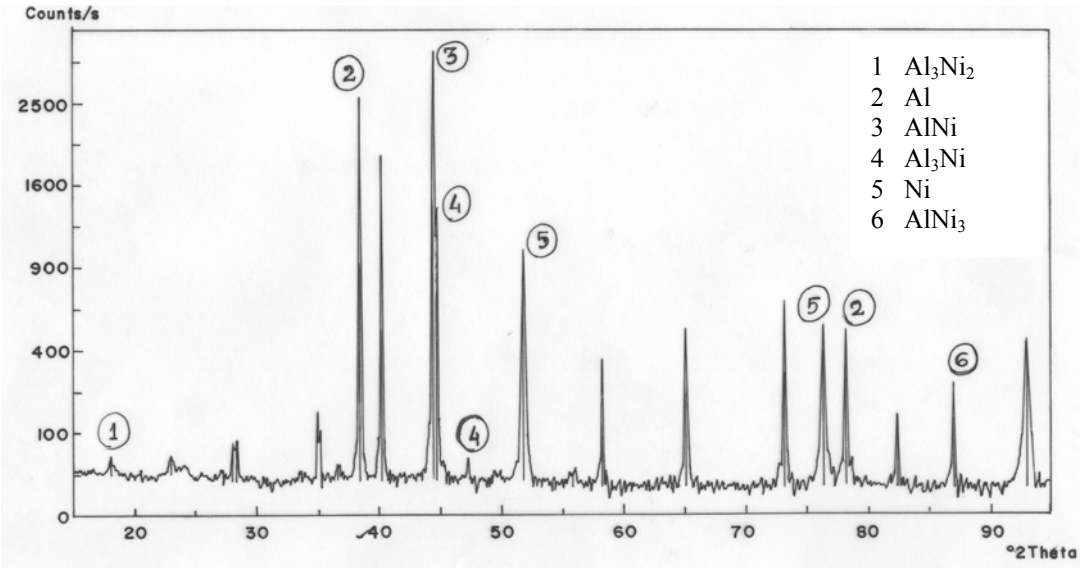

Fig 4.3 X Ray Diffractogram of Ni-Al coating deposited at 10 kW operating power level

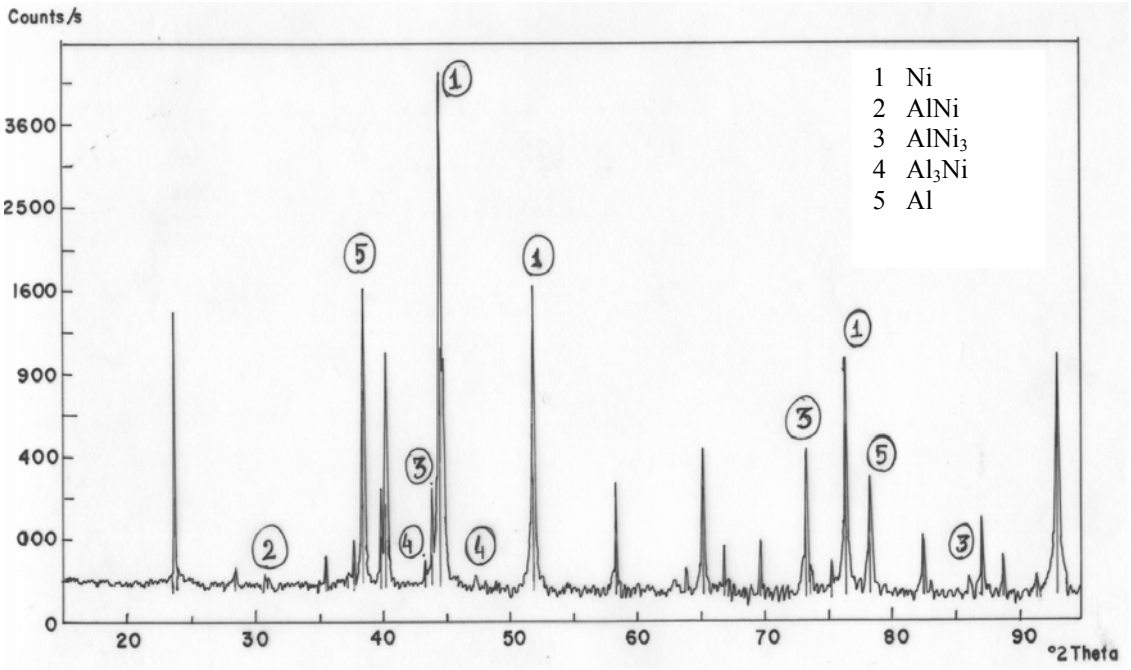

Fig 4.4 X Ray Diffractogram of Ni-Al coating deposited at 20 kW operating power level

Comparing the diffractogrames it can be seen that, the raw powder before spraying contains traces of Al_2O_3 phase; which might be as a consequence of anodic oxidation of aluminum exposed in normal air. The phases observed in the diffractograms of the sprayed coatings are namely, Ni_3Al, Al_3Ni, AlNi etc. Presence of some amount of γ & α-alumina etc. is also observed. This might be due to transformation of Al_2O_3 (which is initially present in the feed stock) during in-flight traverse through the plasma zone. However percentage of the phases has varied with coating deposition parameters. The formation and distribution of these phases in the coating may be one of the reasons for different hardness observed on coatings.

COATING POROSITY

Porosity measurement was done using the image analysis technique. The polished interfaces of various coatings were studied under optical microscope (Neomate) equipped with a CCD camera (JVC, TK 870E). From the digitized image obtained by this system, coating porosity is determined using VOIS image analysis software. The values are given in table 4.3. The amounts of porosity in coatings made at different power level are found to be in the range of 10-13%. It is further noted that the porosity is relatively more in the case of coatings made at lower power level i.e. at 10 kW and also at higher power level i.e. at 24 kW.

Power Level	% of Porosity
10	11.36
12	11.57
16	12.22
20	12.26
24	12.56

Table 4.3 Coating porosity at different power levels

It may be mentioned that in the conventional plasma sprayed coatings, porosity of about 2 – 12 % is generally observed. Thus the values obtained in the coatings under study supports to the soundness of the coating.

COATING MORPHOLOGY

The micrograph of the nickel-aluminide i.e. Ni-Al ball milled powder (feed stock) is shown in Figure 4.5. The variation in particle shape and size is observed. Particles are irregular in shpe, some are elongated also. The micrographs of the Ni-Al mix powders processed at 10kW and 20kW power, collected at 100mm standoff distance is shown in Figures 4.6 (a) & (b) respectively. Comparing these two figures, it is found that, there is an appreciable change in shape and dimension of the particles. This may be due to the fact that, with increased power level during spray deposition, more no. of particles attains melting temperature and hence take a spherical shape during solidification from molten stage in in-flight traverse through plasma. This affects the coating quality and properties.

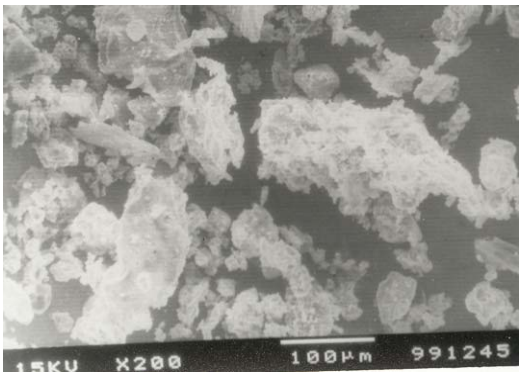

Fig.4.5 Surface morphology of Ni-Al powders, after ball Milling.

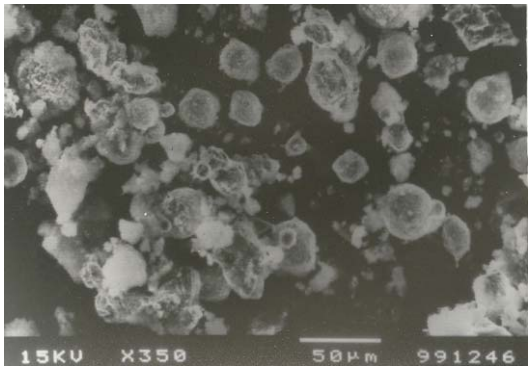

Fig.4.6 (a) Surface morphology of Ni-Al spheroidised powders, Processed at 10kW power level, 100mmTBD.

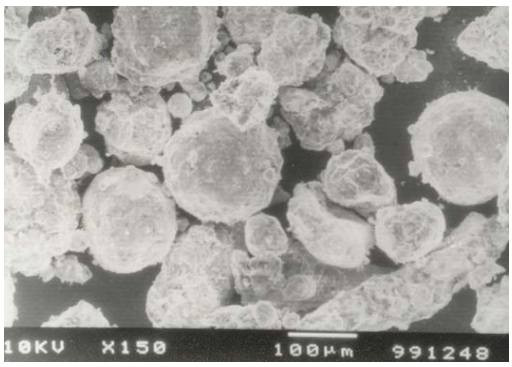

Fig.4.6 (b) Surface morphology of Ni-Al spheroidised powders, processed at 20kW power level, 100mm TBD.

The typical surface morphology of the coatings deposited at different power levels are shown in fig 4.7. It can be seen that the surface morphology of the coatings differ with deposition condition i.e. affected by operating parameters of the plasma torch.

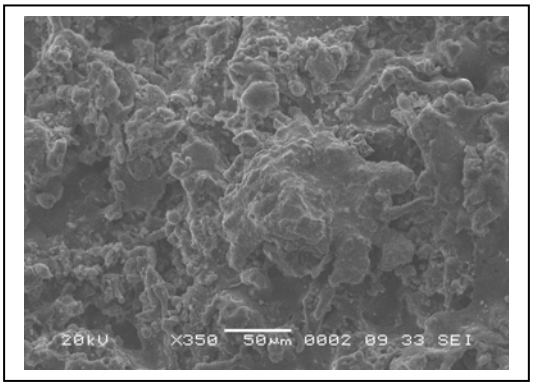

(a)

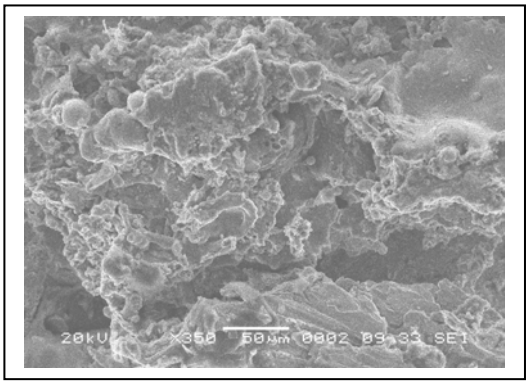

(b)

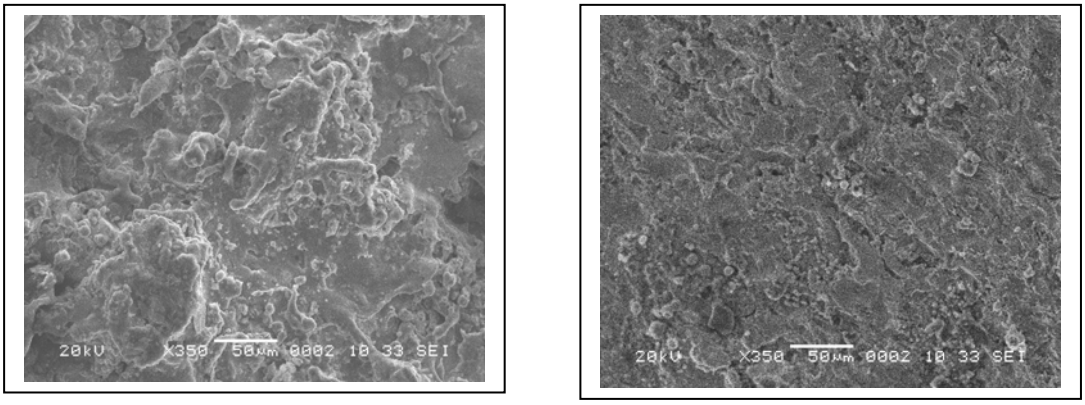

(c) **(d)**

Fig. 4.7 Surface morphology of the coatings deposited at (a) 10kW, (b) 16kW, (c) 20kW and (d) 24kW.

DISCUSSION

In thermal spray coatings developed using atmospheric plasma spray (APS) technique; particle deposition is influenced mainly by the input power to the plasma torch. With increase in power level, the plasma density increases leading to a rise in enthalpy and thereby, the particle temperature. Hence more number of particles gets melted during their in-flight traverse through plasma jet. When these molten species hit the substrate, they get flattened and adhere to the surface. The deposition of layers is favoured with availability of more number of molten / semi molten particles which is enhanced by increasing the torch input power. But, beyond certain limit of operating power level; fragmentation and vaporization of sprayed particles do occur simultaneously and for these two reasons, some (powder) particles fly off during spraying restricting further increase in coating deposition.

The analysis of coating - substrate bond strength of all the sprayed materials on different substrates, presented in table 4.1 envisages that there is an increase in adhesion strength with increase in plasma torch operating power (up to 20 kW) for both the substrates and then takes a decreasing trend. As already mentioned, with increase in torch operating power, there is availability of more number of molten/ semi molten particles which on hitting the substrate, get fused and flattened at a relatively faster rate improving the mechanical inter-locking on the substrate and thereby increasing the bond strength . It has been known that, for a given material, the final coating properties depend on the velocity, temperature and type of particles

just before impact on the substrate or on the coating layers already deposited. The plasma power effectively changes the temperature and particle velocity and therefore affects the coating properties. The composition of the coating materials also affects the coating adhesion strength due to transformation / formation of phases and inter-oxides/inter-metallic compounds that favour the inter particle bonding and adhesion to the substrate. In this investigation, higher adhesion strength in substrates of lower thermal conductivity (i.e. in mild steel) is observed. It is known that the thermal spray coatings adhere weakly to a substrate of high thermal conductivity owing to a low contact angle of the molten droplets (of the sprayed powers) at substrate contact temperature [**156**]. Hence the relatively lower adhesion strength on copper substrates as compared to mild steel substrate is justified.

Micro-hardness measurement is made on optically distinguishable phases present in the coatings. The hardness values are different for different phases and appear to be not much dependent on torch operating power level. On referring to the x ray diffractograms taken on raw material and coated samples, it becomes evident that during coating deposition, formation and transformation of phases have taken place. So during spraying, the phase transformation and/or formation of different phases corroborate to different micro-hardness values obtained on various phases of the coatings.

****

Chapter 5

COATING PERFORMANCE EVALUATION: RESULTS & ANALYSIS

CHAPTER 5

COATING PERFORMANCE EVALUATION: RESULTS AND ANALYSIS

INTRODUCTION

This chapter deals with the analysis of tribological performance of the coatings. It also reports the efficiency of coating deposition under various plasma spraying conditions. The calculated deposition efficiency values form a database which is used for further prediction by neural computation. This chapter also presents the results of the solid particle erosion test conducted on the coated samples. The results give an insight to the performance of the coating in an erosive environment. Artificial neural network analysis is employed and a prediction model is proposed for erosion wear rate as well. Correlation between important control factors and the wear rate has been established.

COATING DEPOSITION EFFICIENCY

Coating deposition efficiency is defined as the ratio of the weight of coating deposited on the substrate to the weight of the expended feedstock. Weighing method is accepted widely to measure this. It can be described by the following equation [**151**].

$$\eta = (G_c/G_p) \text{ X } 100 \ \%$$

Where η is the deposition efficiency, Gc is the weight of coating deposited on the substrate and Gp is the weight expended feed stock.

Deposition efficiency of any coating is a characteristic which not only rates the effectiveness of the spraying method but also is a measure of the coatability of the material under study. Variation of nickel–aluminide coating deposition efficiency on mild steel and copper substrates with operating power level is presented in fig.5.1. It is noted that the efficiency of nickel-aluminum coating deposition, in case of both the substrates, increases in a sigmoidal

fashion with the torch input power. For example: on mild steel substrates, the value increases from 22% to 54% (with input power to plasma torch increasing from 10 kW to 24 kW). Similarly, deposited on copper substrate, the efficiency of deposition is seen to vary from 34% to 57%. Within the domain of experiments carried out in this work, maximum deposition efficiency of 57 % is obtained for coatings made at 24 kW operating power level of the plasma torch (on copper substrate). The maximum deposition efficiencies in case of copper and mild steel substrates are found out to be 54% and 57% respectively.

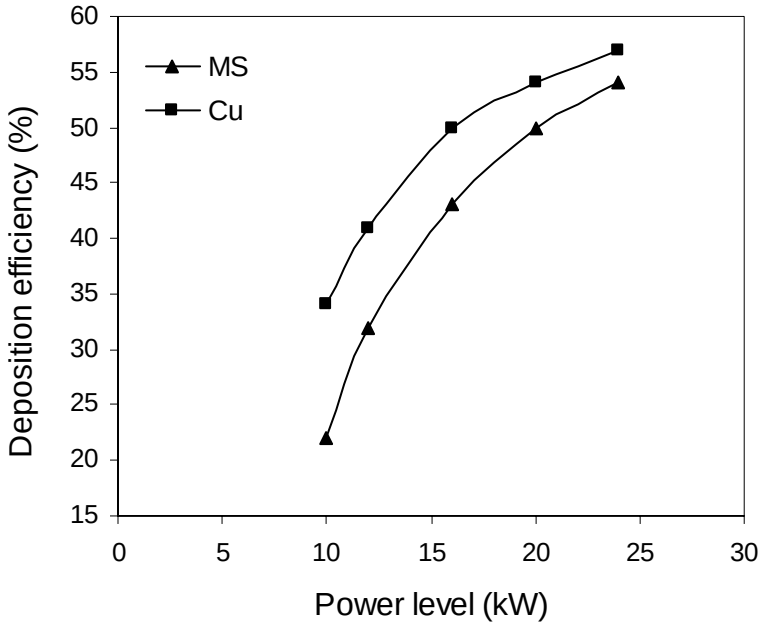

Fig. 5.1 Deposition Efficiency of Ni-Al on MS and Cu substrates

Neural Computation

Coating deposition by plasma spraying is considered as a non-linear process with respect to its variables: either materials or operating conditions. To obtain functional coatings exhibiting selected in-service properties, combinations of processing parameters have to be planned. These combinations differ by their influence on the coating properties and characteristics. In order to control the spraying process, one of the challenges nowadays is to recognize parameter interdependencies, correlations and individual effects on coating characteristics. Neural computation can be used to study these interrelated effects. In the present work, influence of plasma torch input power on coating deposition efficiency has been studied. A

methodology based on artificial neural networks (ANN) is used that involves database training to predict property-parameter evolutions. This section presents the database construction, implementation protocol and a set of predicted results related to the coating deposition efficiency. The details of this methodology are described by Rajasekaran and Pai [**157**].

ANN Model: Development and Implementation

An ANN is a computational system that simulates the microstructure (neurons) of biological nervous system. The most basic components of ANN are modeled after the structure of brain. Inspired by these biological neurons, ANN is composed of simple elements operating in parallel. It is simple clustering of the primitive artificial neurons. This clustering occurs by creating layers, which are then connected to another. The multi layer neural network has been utilized in the most of the research works for material science. The database is built considering experiments at the limit ranges of each parameter. Experimental result sets are used to train the ANN in order to understand the input-output correlations. The database is then divided into three categories, namely: (i) a validation category, which is required to define the ANN architecture and adjust the number of neurons for each layer. (ii) a training category, which is exclusively used to adjust the network weights and (iii) a test category , which corresponds to the set that validates the results of the training protocol. The input variables are normalized so as to lie in the same range group of 0-1.

Input Parameters for Training	**Values**
Error tolerance	0.0001
Learning parameter(ß)	0.1
Momentum parameter(α)	0.002
Noise factor **(NF)**	0.0001
Maximum cycles for simulations	2000,000
Slope parameter (£)	0.6
Number of hidden layer	6
Number of input layer neuron **(I)**	2
Number of output layer neuron **(O)**	1

Table 5.1 Input parameters selected for training

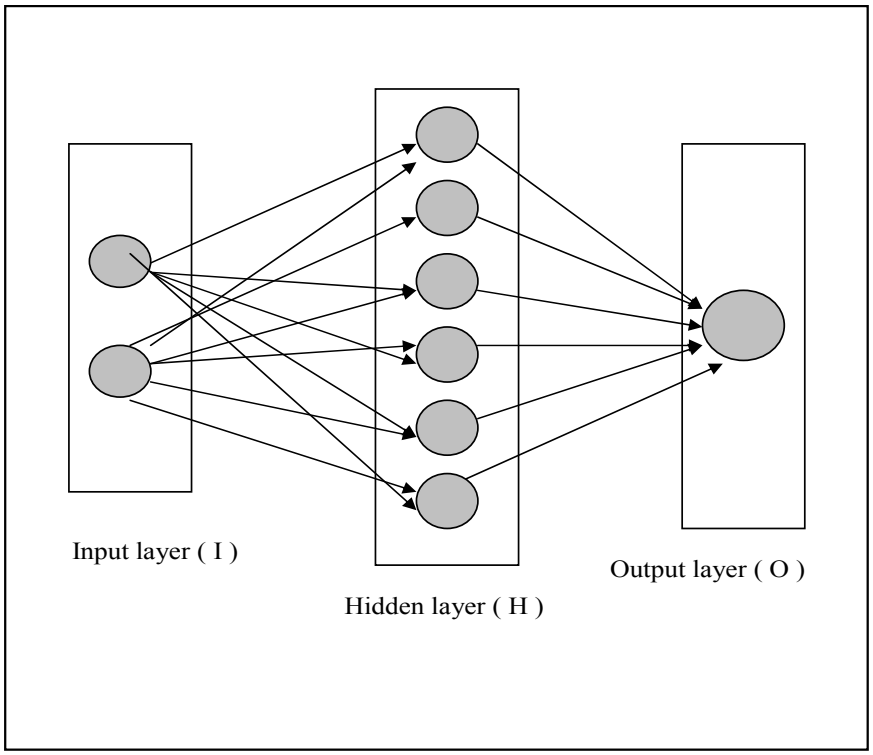

Fig. 5.2 The three layer neural network

To train the neural network used for this work, about 30 data sets of different coatings applied on selected substrates are taken. It is ensured that these extensive data sets represent all possible input variations within the experimental domain. So a network that is trained with this data is expected to be capable of simulating the plasma spray process. Different ANN structures (I-H-O) with varying number of neurons in the hidden layer are tested at constant cycles, learning rate, error tolerance, momentum parameter and noise factor and slope parameter. Based on least error criterion, one structure, shown in table 5.1, is selected for training of the input-output data. The learning rate is varied in the range of 0.001-0.100 during the training of the input-output data. The network optimization process (training and testing) is conducted for 2000,000 cycles for which stabilization of the error is obtained. Neuron numbers in the hidden layer is varied and in the optimized structure of the network, this number is 6. The number of cycles selected during training is high enough so that the ANN models could be rigorously trained. A software package NEURALNET for neural computing developed by Rao and Rao [**158**] using back propagation algorithm is used as the prediction tool for coating deposition efficiency at different operating power levels. The three-layer neural network having an input layer (I) with two input nodes, a hidden layer(H)

with six neurons and an output layer (O) with one output node employed for this work is shown in fig. 5.2.

ANN Prediction of Deposition Efficiency

The prediction neural network was tested with tweleve data sets from the original process data. Each data set contained inputs such as torch input power, substrate material and an output value i.e. deposition efficiency was returned by the network. As further evidence of the effectiveness of the model, an arbitrary set of inputs is used in the prediction network. Results were compared to experimental sets that may or may not be considered in the training or in the test procedures. Fig. 5.3 presents the comparison of predicted output values for deposition efficiency for coatings obtained at various operating power levels with the actual deposition efficiency found experimentally.

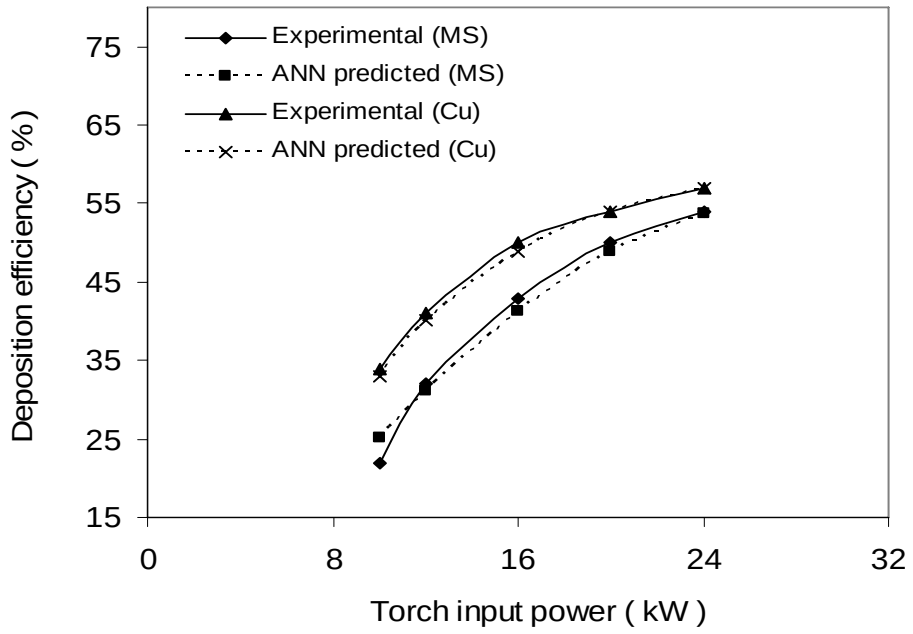

Fig 5.3 Comparison plot for predicted and experimental values of deposition efficiency of Ni-Al coatings on mild steel and copper substrates

It is interesting to note that the predictive results show good agreement with experimental sets realized. The optimized ANN structure further permits to study quantitatively the effect of torch input power on the coating deposition in range larger than the experimental limits, thus offering the possibility to use the ANN in a large parameter space. In the present investigation, this possibility was explored by selecting the torch input power in a range from 6 kW to 30 kW, and sets of predictions for deposition efficiency on all the two substrates are

evolved. Fig. 5.4 illustrates the predicted evolution of deposition efficiencies with respect to torch input power for mild steel and copper substrates.

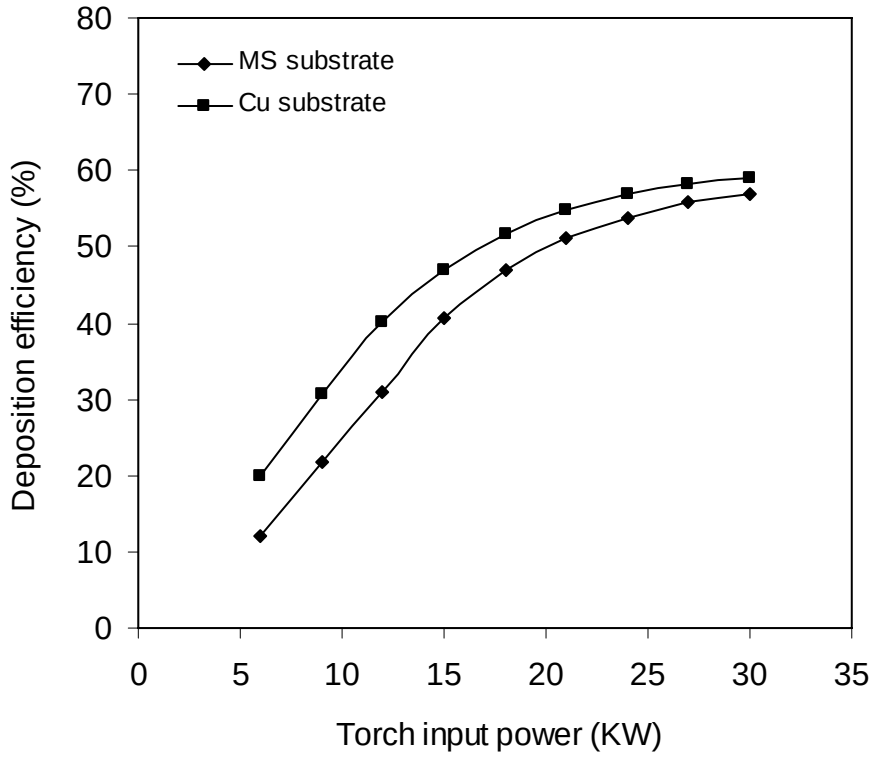

Fig.5.4 Predicted coating deposition efficiency on mild steel and copper substrates

Remarks

The deposition efficiency presents a sigmoid-type evolution with the torch input power (fig. 5.3 and fig. 5.4). As the power level increases, the total and the net available energies increase (the arc current intensity increases from 250A to 480A for operating power increasing from 10 kW to 24 kW). This leads to a better in-flight particle molten state and hence to higher probability for particles to flatten. The deposition efficiency reaches a plateau for the highest current levels due to the plasma jet temperature increasing which in turn increases both the particle vaporization ratio and the plasma jet viscosity.

Functional coatings have to fulfill various requirements. The deposition efficiency is one the main requirements of the coatings developed by plasma spraying. It represents the effectiveness of the deposition process as well as the coatability of the powders under study. Neural computation can be used as a tool to process very large data related to a spraying

process and to predict coating characteristic such as deposition efficiency, the simulation can be extended to a parameter space larger than the domain of experimentation.

SOLID PARTICLE EROSION WEAR BEHAVIOUR

Solid particle erosion is a wear process where particles strike against a surface and promote material loss. During flight, a particle carries momentum and kinetic energy, which can be dissipated during impact due to its interaction with a target surface. In case of plasma spray coatings encountering such situations, no specific model has been developed and thus the study of their erosion behavior has been mostly experimental data **[139**]. In this work, room temperature solid particle erosion trials on a few selected coatings (made at 20kW on mild steel) are carried out using a compressed air blasting type rig. Detailed description of the test is given in Chapter 3.

Rate of erosion of the nickel-aluminide coatings varies with the erodent dose. At a specified feed rate of the erodent, the cumulative mass of erodent changes as the time of exposure advances. Erosion tests were conducted for three different impact velocities (31.2, 44.2 and 58.5 m/s), five impact angles (15, 30, 45, 60 and 90 degrees) and two stand-off-distances (100 and 150mm). The variations of the coating wear rates with the erodent mass are illustrated in figures 5.5 to 5.10.

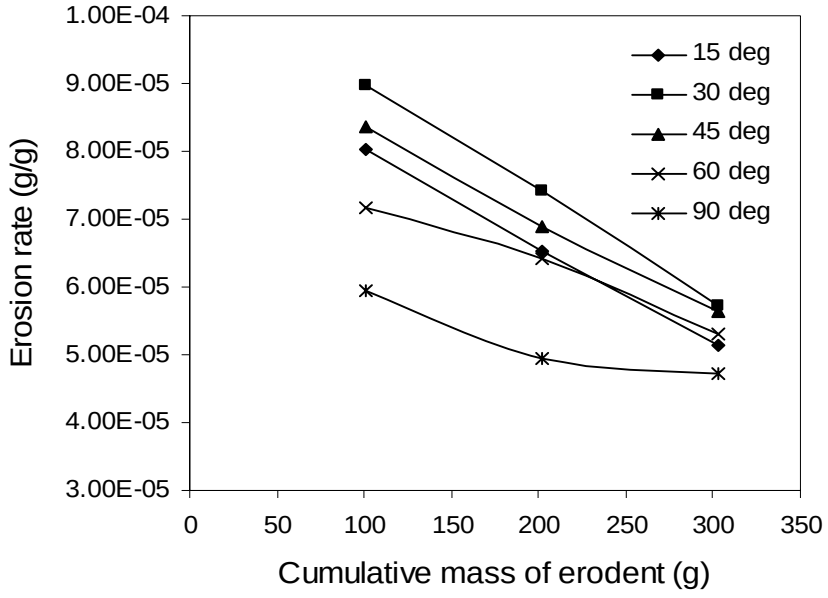

Fig. 5.5 Erosion rate Vs cumulative mass of erodent (impact vel. 31.2m/s, SOD = 100 mm)

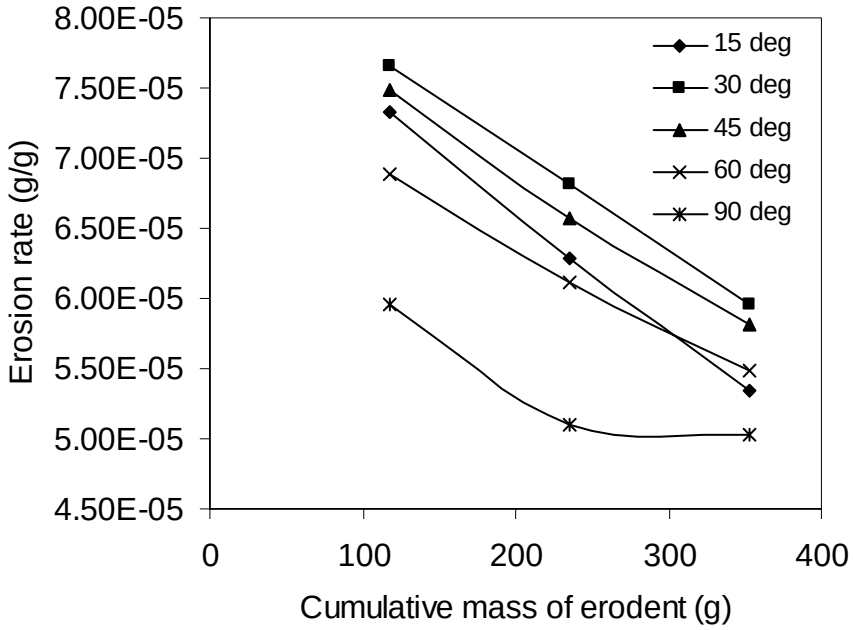

Fig. 5.6 Erosion rate Vs cumulative mass of erodent (impact vel. 44.2 m/s, SOD = 100 mm)

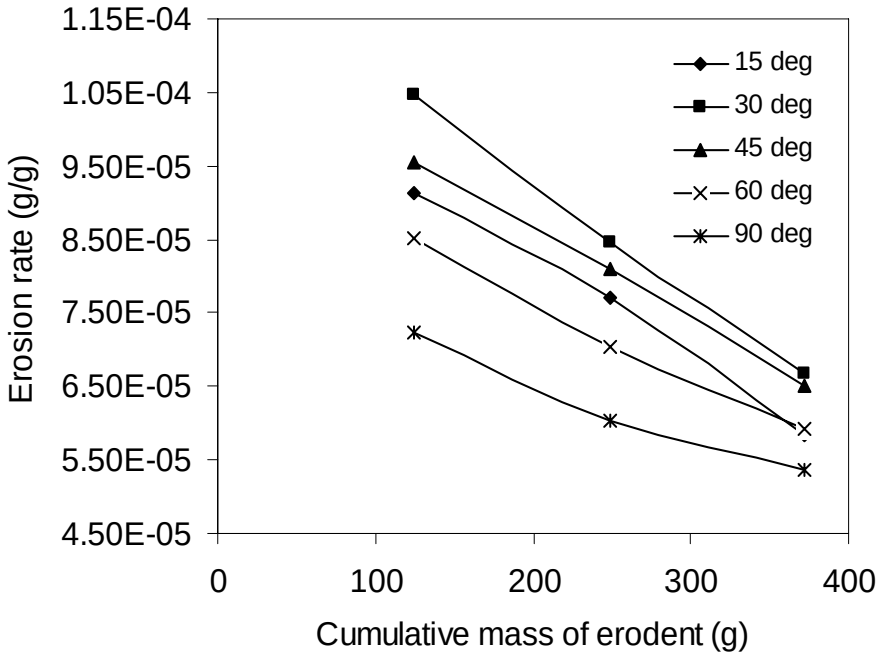

Fig. 5.7 Erosion rate Vs cumulative mass of erodent (impact vel. 58.5 m/s, SOD = 100 mm)

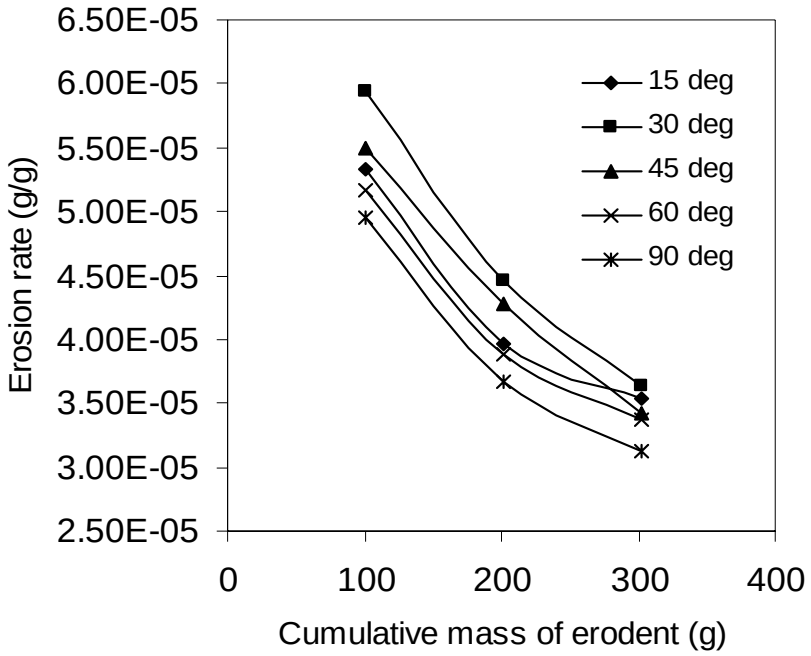

Fig. 5.8 Erosion rate Vs cumulative mass of erodent (impact vel. 31.2m/s, SOD = 100 mm)

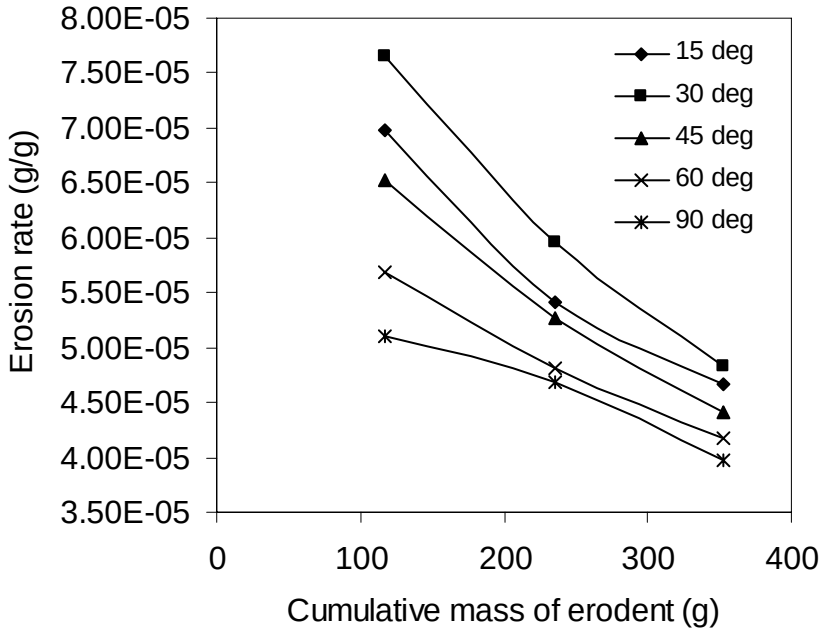

Fig. 5.9 Erosion rate Vs cumulative mass of erodent (impact vel. 44.2m/s, SOD = 150 mm)

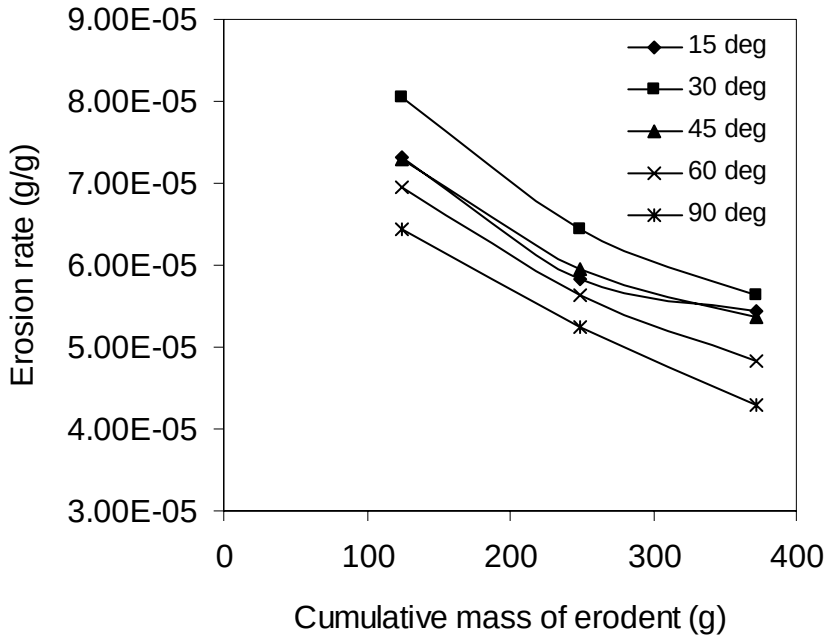

Fig. 5.10 Erosion rate Vs cumulative mass of erodent (impact vel. 58.5 m/s, SOD = 150 mm)

The decrease in the wear rate of various plasma sprayed coatings with erosion time (or erodent dose) has been reported earlier by Levy [**159**]. He has shown that, the incremental erosion rate curves of a large number of materials start with a high rate at the first measurable amount of erosion and then decreases to a much lower steady state value [**160**] . In this work, similar trend is found in nickel-aluminide coatings subjected to erosion at various impact angles. This can be attributed to the fact that the fine protrusions on the coating parts are relatively loose and can be removed with less energy than what would be necessary to remove a similar part from the bulk of the coating. Consequently, the initial wear rate is high. With increasing exposure time the rate of wear starts decreasing and in the transient erosion regime, a sharp drop in the wear rate is obtained. As the coating surface gradually gets smoothened, the rate of erosion becomes almost steady.

The rate of erosion of the coating is also found to be greatly affected by the angle of impingement of the eroding particles. Figures 5.11 and 5.12 show the variation of erosion wear rate with the angle of impact at different impact speeds and stand-off distances. It is seen that initially with increase in impact angle the erosion rate increases, but beyond 30^0 the rate keeps decreasing monotonically. This trend is similar for different impact speeds and stand-off distances.

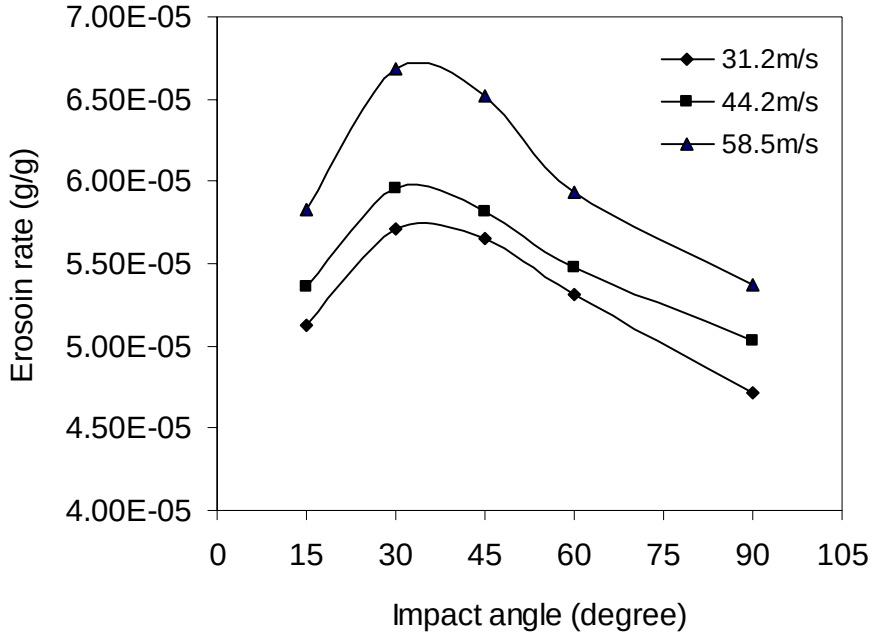

Fig. 5.11 Erosion rate Vs. angle of impact at different impact velocities (exposure time = 6 minutes , SOD = 100 mm]

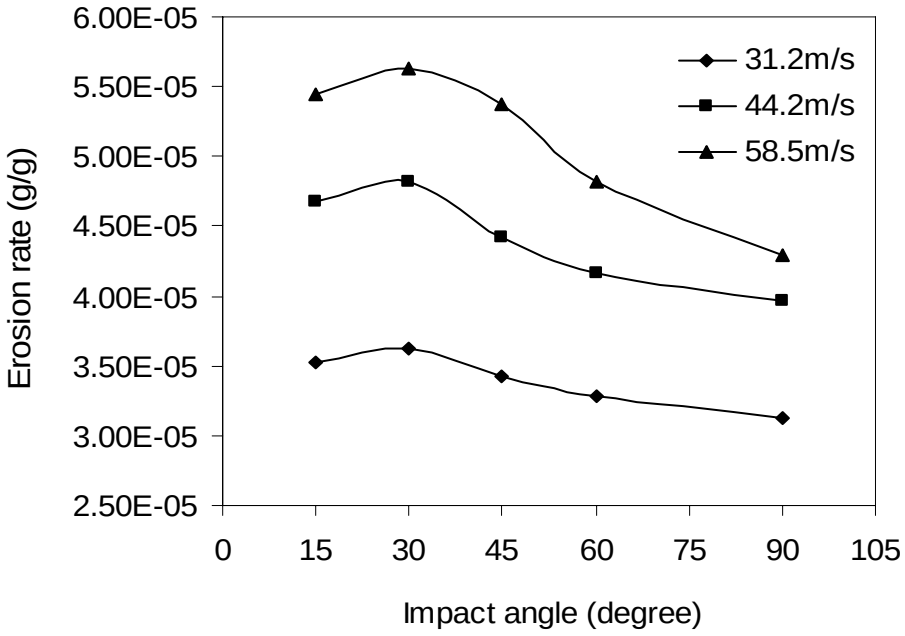

Fig. 5.12 Erosion rate Vs. angle of impact at different impact velocities (exposure time = 6 minutes , SOD = 150 mm]

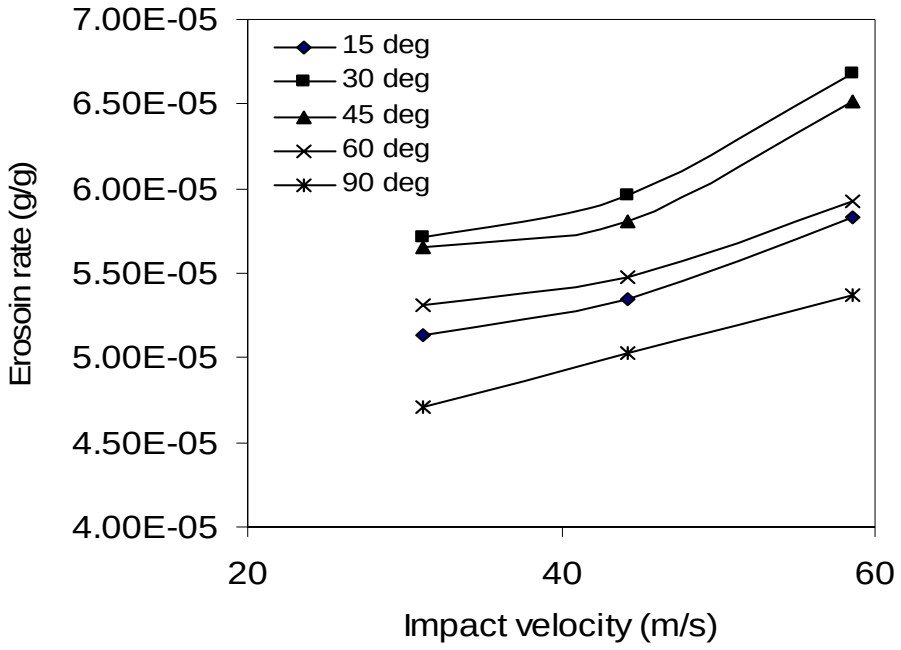

Fig. 5.13 Erosion rate Vs. Impact velocity at different impact angles
(Exposure time = 6 minutes , SOD = 100 mm)

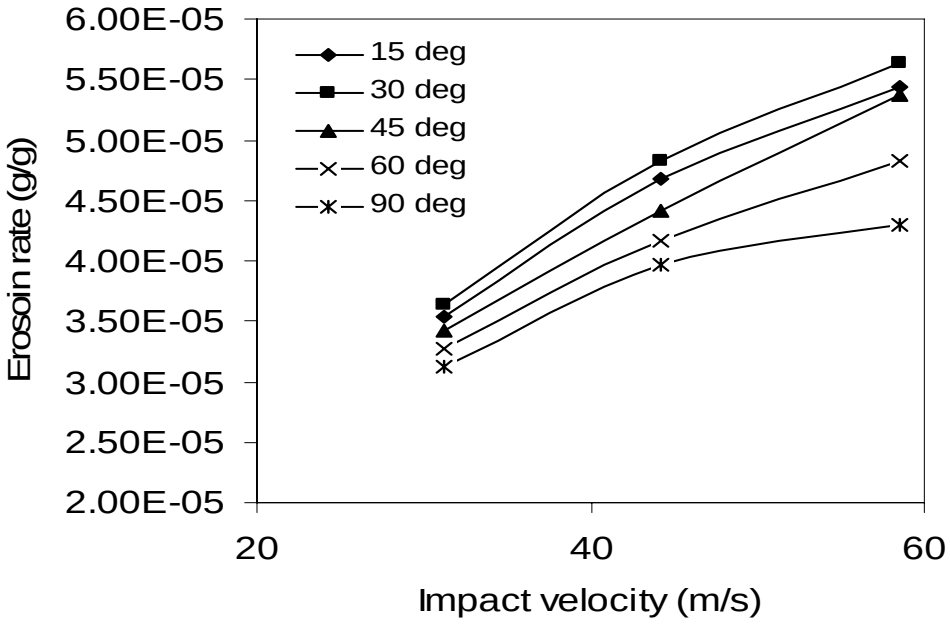

Fig. 5.14 Erosion rate Vs. Impact velocity at different impact angles
(Exposure time = 6 minutes, SOD = 150 mm)

It is evident from figures 5.13 and 5.14 that the effect of impact velocity on coating erosion is also very significant. It is seen that with increase in the impingement velocity the coating mass loss due to erosion increases. This trend is found for different impact angles and stand-off distances.

ANN Implementation in Prediction of Erosion Wear Rate

Neural computation is used to predict erosion rate of nickel-aluminide coating. The network is trained with the database generated from experimental results by taking suitable input parameters for training. Prediction results are compared to experimental sets. Figures 5.15, 5.16 and 5.17 present the comparison of predicted output values for erosion rate obtained at various impact angles with the actual values found experimentally at different impact speeds.

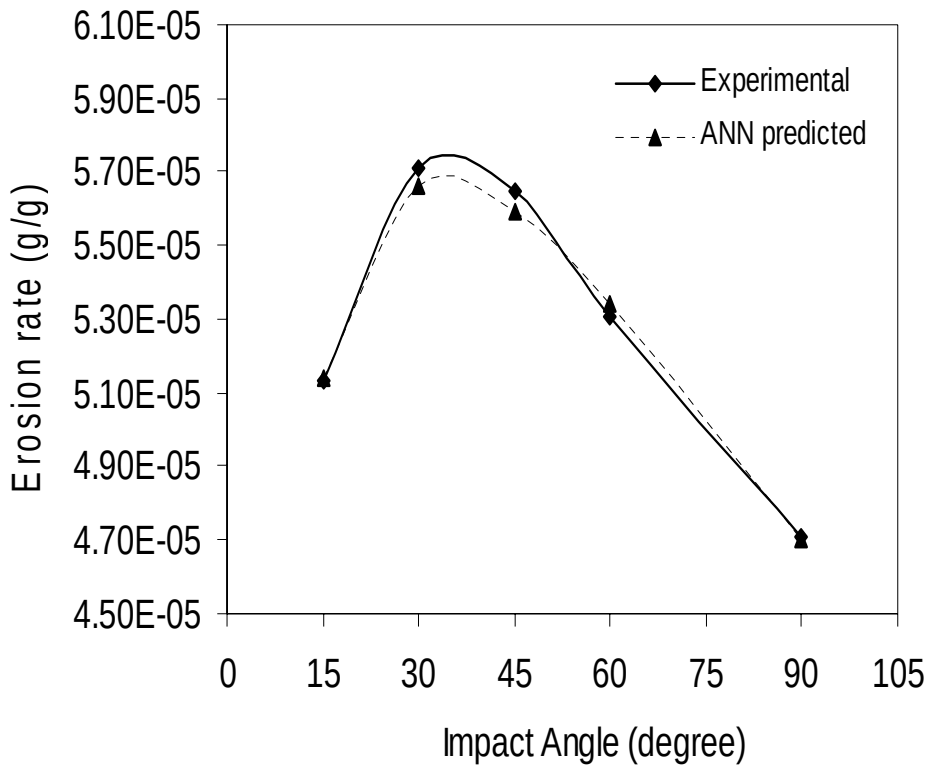

Fig.5.15 Comparison plot for predicted and experimental values of Erosion rate [Impact velocity =31.2m/s SOD = 100 mm]

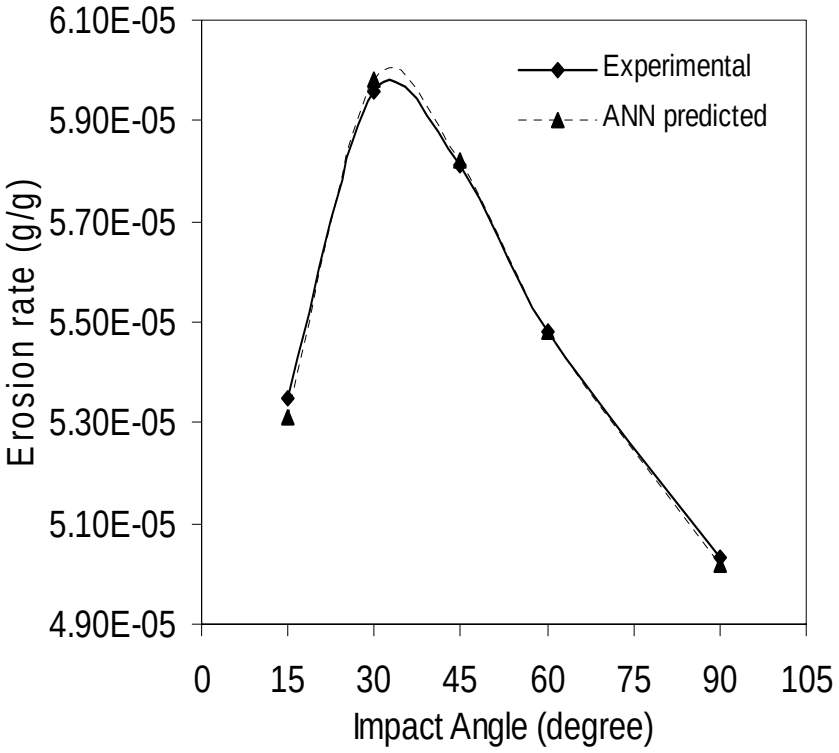

Fig.5.16 Comparison plot for predicted and experimental values of Erosion rate [Impact velocity =44.2m/s SOD = 100 mm]

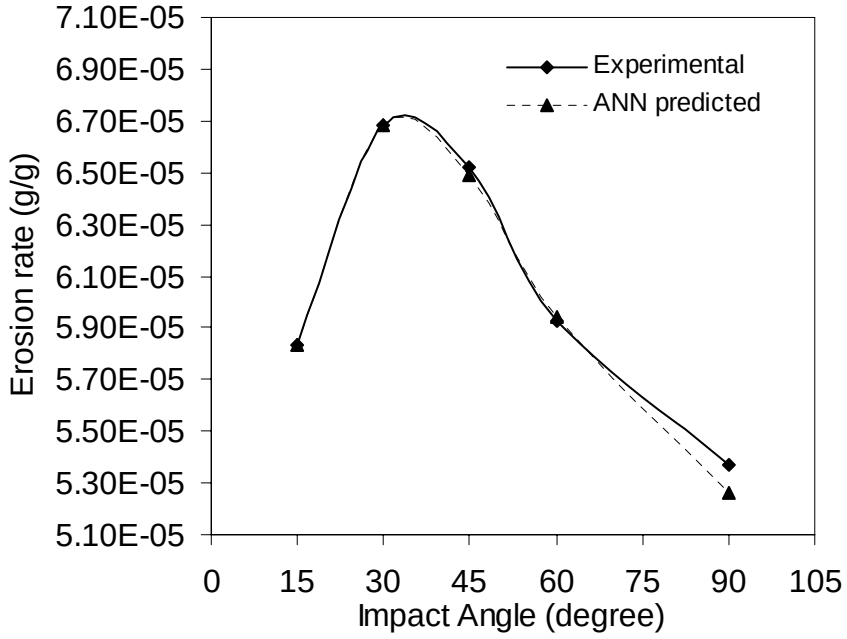

Fig.5.17 Comparison plot for predicted and experimental values of Erosion rate [Impact velocity =58.5m/s SOD = 100 mm]

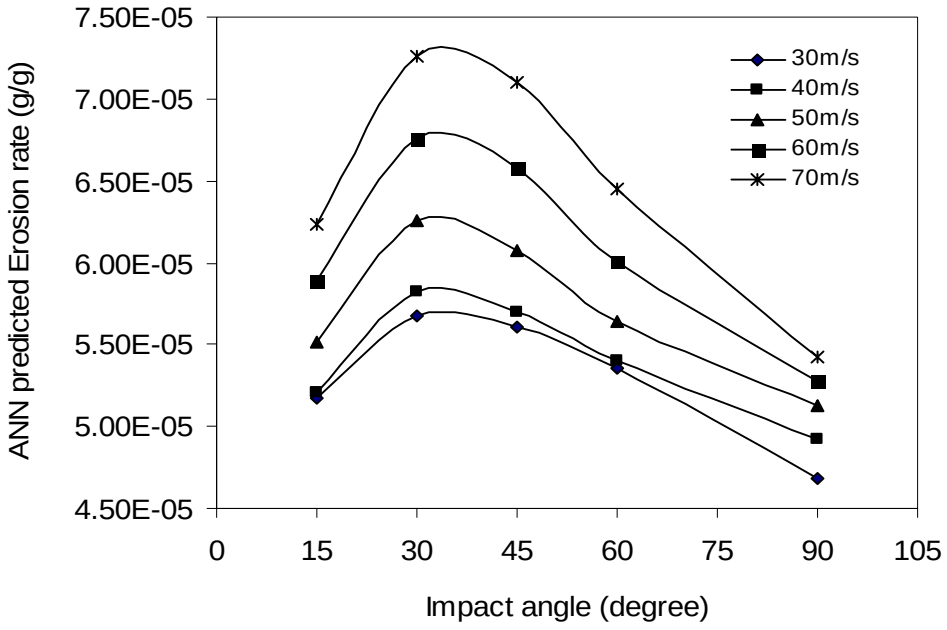

Fig.5.18 Predicted Erosion rate for different impact velocities with impact angle
SOD = 100mm

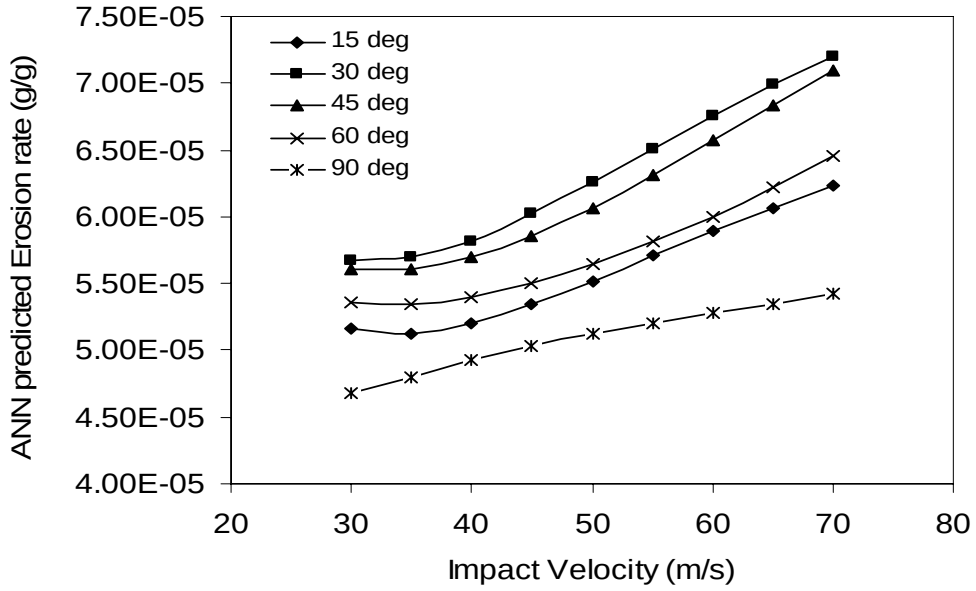

Fig.5.19 Predicted Erosion rate for different impact angles with impact velocity
SOD = 100mm

It is interesting to note that the predictive results show good agreement with experimental sets. The optimized ANN structure further permits to study the effect of impact angle and velocity on the coating erosion in a domain larger than the experimental limits. Figures 5.18 and 5.19 illustrate the predicted evolution of erosion rate with impact angle and impact velocity.

Correlation between Erosion Wear Rate, Impact Velocity and Impact Angle

In this study, an attempt is made to derive a correlation of the control factors for quantifying the erosion rate. The single-objective quantitative determination of the relationship between coating erosion rate and two important control factors i.e. impact velocity and the angle of impingement has been found out using non-linear regression analysis with the help of SYSTAT 7 software. For erosion rate **E** in terms of impact velocity (**V**) and angle of impact (α), the following mathematical model is suggested.

$$E = KV^{n}(\sin^{m}\alpha)$$

Here, E is the performance output terms and **K, m and n** are the model constants. From regression analysis, the constant are found out to be

$$K = 2.512 \times 10^{-5}$$

$$m = -0.031$$

$$n = 0.209$$

This makes the equation as follows:

$$E = 2.512 \times 10^{-5} V\ 0.209\ (\sin \alpha)^{-0.031}$$

The correctness of the calculated constants is confirmed as high correlation coefficients (r^2) in the tune of 0.96 are obtained for the equation and therefore, the model is quite suitable to be used for further analysis.

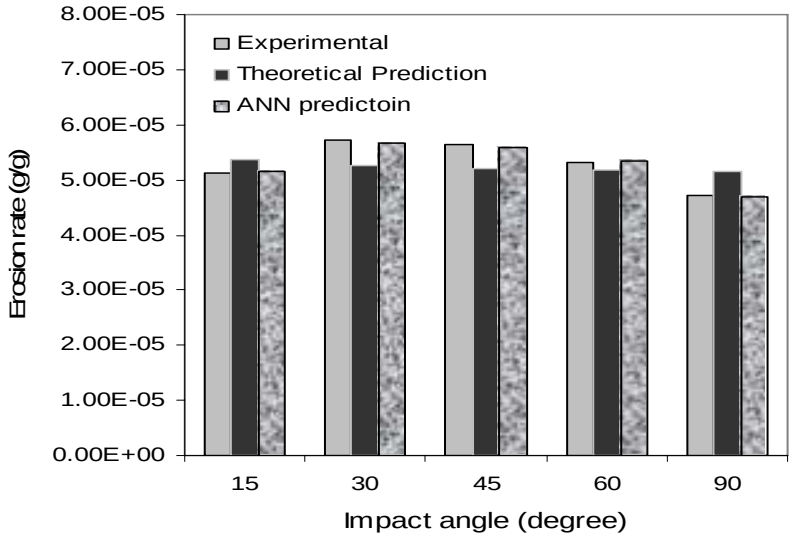

Fig.5.20 Comparison plot for predicted, formula and experimental values of Erosion rate [Impact velocity =31.2m/s SOD = 100 mm]

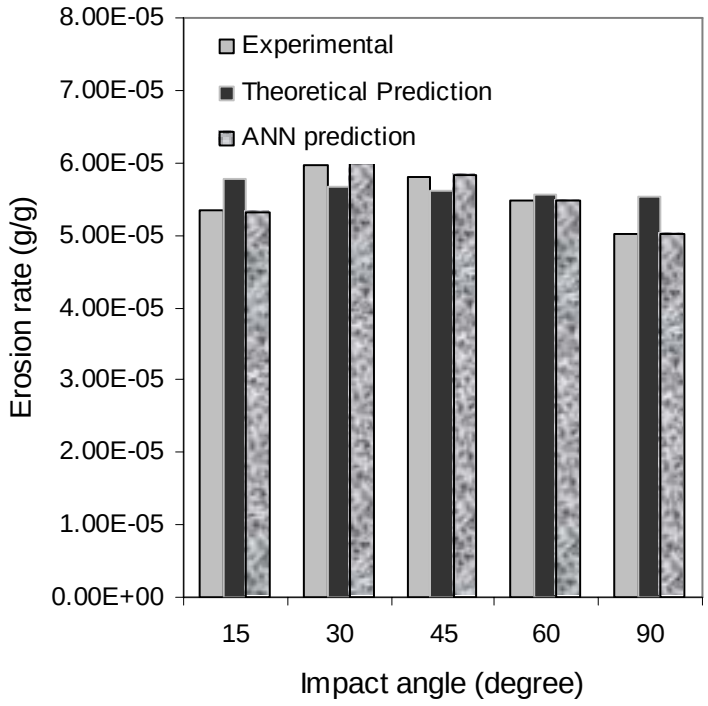

Fig.5.21 Comparison plot for predicted, formula and experimental values of Erosion rate [Impact velocity =44.2m/s SOD = 100 mm]

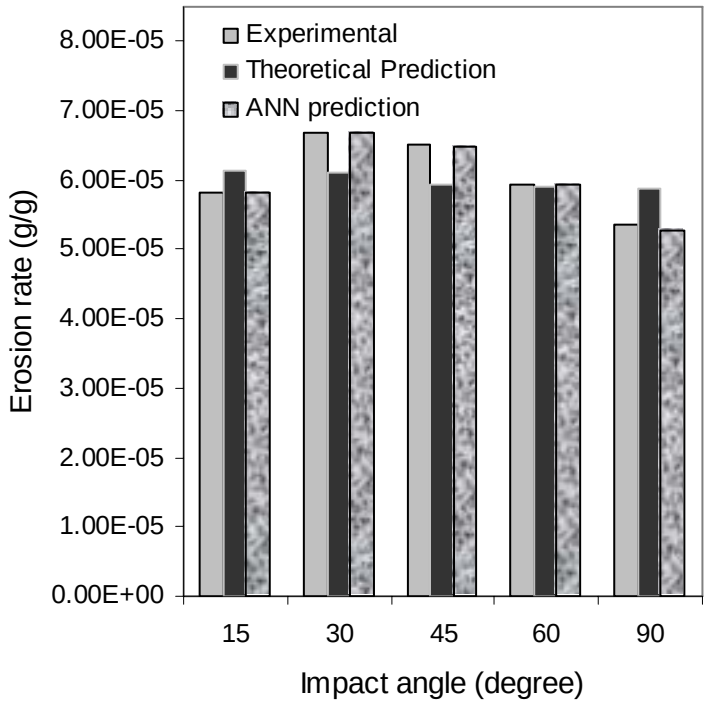

Fig.5.22 Comparison plot for predicted, formula and experimental values of Erosion rate [Impact velocity =58.5m/s SOD = 100 mm]

Impact angle (degree)	Impact velocity (m/s)	Erosion rate ($x10^{-5}$g/g)		% Error
		Expt.Value	Calculated Value	
15	31.2	5.13	5.37	4.67
30	31.2	5.71	5.26	7.88
45	31.2	5.65	5.21	7.78
60	31.2	5.31	5.17	2.63
90	31.2	4.71	5.15	9.34
15	44.2	5.35	5.78	8.03
30	44.2	5.96	5.66	5.03
45	44.2	5.81	5.61	3.44
60	44.2	5.48	5.57	1.64
90	44.2	5.03	5.54	10.13
15	58.5	5.83	6.13	5.14
30	58.5	6.68	6.01	10.02
45	58.5	6.52	5.94	8.89
60	58.5	5.93	5.91	0.33
90	58.5	5.37	5.88	9.56

Table 5.2 Comparison of experimental, predicted and calculated values of erosion rates with the associated percentage error

Figures 5.20, 5.21 and 5.22 show comparison of the coating erosion rate values predicted by ANN and the values calculated using the suggested correlation with those obtained experimentally at different operational conditions. Table 5.2 presents these values along with the associated percentage error in a tabular form.

It is seen from the comparison plots that the prediction model and the correlation model proposed for the erosion rate are in reasonably good agreement with the experimental data. Thus the models are quite suitable to be used for any further analysis of erosion in plasma sprayed nickel-aluminide coatings.

Remarks

The results presented in fig. 5.11 and 5.12 confirm that the angle at which the stream of solid particles impinges the coating surface influences the rate at which the material is removed. It

further suggests that, this dependency is also influenced by the nature of the coating material. Normally, for brittle materials subjected to erosion, the maximum wear rate occurs at 90^0 impact and for ductile material this is 15^0-30^0. In the present investigation, the peak erosion rate is recorded at 30^0 for the coatings regardless the impact velocity and the stand-off distance. This implies the ductile behaviour of the coating under study. The angle of impact determines the relative magnitude of the two components of the impact velocity namely, the component normal to the surface and parallel to the surface. The normal component will determine how long the impact will last (i.e. contact time) and the load. The product of this contact time and the tangential (parallel) velocity component determines the amount of sliding that takes place. The tangential velocity component also provides a shear loading to the surface, which is in addition to the normal load that the normal velocity component causes. Hence as this angle changes the amount of sliding that takes place also changes as does the nature and magnitude of the stress system. Both of these aspects influence the way a coating wears. These changes imply that different types of material would exhibit different angular dependency.

Branco et al. (**149**) reported that, the coating porosity influences the erosion in three ways. Firstly, it reduces the material strength against plastic deformation or chipping since the material at the edge of a void lacks mechanical support. Secondly, the concave surface inside a void that is not under the shadow of some void edge will see an impinging particle at an angle higher than the average target surface to impact angle (which is detrimental for brittle materials). And finally, pores can impair strength by acting as stress concentrators and/or decreasing the load bearing surface. The coatings under this investigation are though brittle in nature, the effect of pore volume fraction on erosion wear needs a more detailed investigation.

*****

Chapter 6

CONCLUSIONS

CONCLUSIONS

The conclusions drawn from the present work are as follows:

- Mixture of commercial grade nickel and aluminum powder is coatable on metal substrates by thermal plasma spraying technique. These coatings possess desirable coating characteristics such as good adhesion strength, hardness etc.
- During plasma spray deposition, formation of aluminide phases of nickel is observed. Maximum adhesion strength of ~ 12.5 MPa is recorded for these nickel-aluminide coatings on mild steel substrates and ~ 10.15 MPa on copper substrates, at 20kW operating power level of plasma torch.
- Maximum deposition efficiency of ~ 57% is obtained for Ni-Al coatings on copper and ~ 54% on mild steel substrates.
- Operating power level of the plasma torch influences the coating adhesion strength, deposition efficiency and coating hardness to a great extent. The coating morphology is also largely affected by the torch input power.
- Occurrence of phase transformations and formation of aluminide phases such as Ni_3Al, Ni_3Al_2 during plasma spraying is evident. The different aluminide phases observed in XRD studies corroborate to the observation of different hardness values of different optically distinguished phases.
- The coatings developed in this work is harder than that of the substrate materials, Hence, these coatings can be recommended for tribological applications.
- The solid particle erosion wear resistance of these coatings is fairly good. The rate of erosion of the coating is found to be greatly affected by the angle of impact and the velocity of impact of the eroding particles.
- Artificial neural networks can be gainfully employed to simulate property-parameter correlations beyond the experimentation range. The ANN technique can also be used for prediction of coating performance under different operational conditions.

SCOPE FOR FUTURE WORK

The present work opens up a wide scope for future investigators to explore many other aspects of such coatings. Evaluation of thermal stability of these coatings is to be done to find its suitability for high temperature applications. Sliding wear behaviour under different operating conditions is to be investigated. Effect of addition of other elements with Ni+Al powder for deposition to produce higher interface bond strength can be investigated.

*****

References

References

1 P. R. Taylor -- *Thermal Plasma Processing of Materials*— Power Beams and Materials Processing PBAMP 2002, Ed. A.K. Das et al., Allied Publishers Pvt. Ltd., Mumbai, India, pp. 13-20 (**2002**)

2 P.P.Bandopadhyaya- *Processing and Characterization of Plasma Sprayed Ceramic Coatings on Steel Substrate*—Ph.D. Thesis , IIT, Kharagpur, India (**2000**)

3 J. Z. Chen, H. Herman and S. Safai, Evaluation of NiAl and NiAl-B Deposited by Vacuum Plasma Spray, J. Thermal Spray Technology, 2,(1993),357.

4 C. T. Liu and V. K. Sikka, Nickel Aluminides for Structural Uses, J. of Metals, 38,(1986),13.

5 H. Ito,M. Umakoshi, R. Nakamura, T. Yokoyama, K. Urayama and M.Kato, Proc. Fourth Nat. Thermal Spray Conf., Pittsburgh,PA, USA,(1991),405.

6 D.A.Gerdeman, N.L.Hecht, Arc Plasma Technology in Material Science, Springer, Berlin (1972)

7 R.B. Heiman, '*Plasma Spray Coating, Principle and Application'*, VCH, Weinheim, Germany, **1996**.

8 R. Edwards, Cutting Tools, The Institute of Materials, UK, **1993**.

9 K. G. Budinski, *Surface Engg. For Wear Resistance*, N.J., USA, **1988**.

10 K. N. Stratford, **1984**, *Coatings and Surface Treatments for Corrosion and Wear Resistance*, Inst. Of Corrosion Sc. And Tech., Birmingham, UK.

11 L. J. Durney, **1984**, Electroplating Engineering Handbook, Van Norstand, NY, USA.

12 T. Biestek and J. Weber, **1976**, *Electrolytic and Chemical Conversion Coating*, Portcullis Press Ltd, Warsaw, Poland.

13 N. A. Tape, E. A. Baker and B. C. Jackson, **1976**, *Plating and Surface Finishing*, October, p 30.

14 N. Fieldstein, **1981**, Materials Engg., July, P 38.

15 C. F. Spencer, **1975**, Metal Finishing, January, p 38.

16 J. Mcdermott, **1972**, *Electroless Plating and Coating of Metals*, Noyes Data Corp, NJ., USA.

17 M. F. Ashby and D. R. H. Jones, **1980**, Engineering Materials, Pergamon press, NY, USA.

18 C. R. Brooks, **1979**, *Heat Treatment of Ferrous Metals*, Hemisphere Publishing Co., Washington, USA.

19 C. Dawes and D. F. Tranter, **1983**, Metal Progress, December, p 17.

20 A. V. Linial and H. E. Hunterman, **1979**, *Wear of Materials*, ASME, NY, USA.

21 S. Bhattacharya and F. D. Seaman, **1985**, *Laser Heat Treatment for Gear Application in "Laser Processing of Materials*", The Metallurgical. Soc. Of AIME, p 211.

22 F. A. Smidt, **1983**, *Ion Implantation for Material Processing*, Noyes Data Corp, NJ, USA.

23 R. F. Bunshah, **1982**, *Deposition Technologies for Films and Coatings*, Noyes Publications, NJ, USA.

24 J. Vossen and W.Kern, **1978**, *Thin Film Processes*, Academic Press, NY, USA.

25 H. S. Legg and K. O. Legg, **1989**, *Ion Beam Based Techniques for Surface Modification in "Surface Modification Technologies*", by T.S. Sudarsan (ed), Marcell Dekker Inc, USA, p 219.

26 J. M. Blocher, **1966**, *Vapour Deposited Materials in "Vapour Deposition*", by C. F. Powell, J. H. Oxley and J. M. Blocher (eds), Willwy, NY, USA.

27 D. G. Bhatt, **1989**, *Chemical Vapour Deposition, in "Surface Modification Technologies*", by T. S. Sudarsan (ed), Marcell Dekker Inc, USA, p 141.

28 R. L. Little, **1979**, *Welding and Welding Technology*, TMH Publications, New Delhi, India.

29 The Welding Handbook, **1980**, American Welding Soc., USA.

30 P. T. Houldcroft, **1967**, *Welding Process Tech*., Welding Process Tech., Cambridge Univ Press, UK.

31 L. F. Longo, **1985**, *Thermal Spray Coatings*, ASM, USA.

32 V. Meringolo, **1983**, *Thermal Spray Coating*, Tappi Press, Atlanta, USA.

33 J. L. Morris, **1951**, *Welding Principle for Engineers*, Prentice Hall, USA.

34 L. Powloski, **1995**, *The Sc. And Engg. Of Thermal Spraying*, Willey, USA.

35 E. Lugscheider, **1992**, Technica, v 19, p 19.

36 D. G. McCartney, **1998**, Surf. Engg., v 14(2), p 204.

37 V. V.Sobolev, J.M. Guilemany, J. Nutting and J.R. Miquel, **1997**, Int. Mat. Rev, v 42(3), p117.

38 B. Xu, M. Shinning and J. Wang, **1995**, Surf. Engg., v11(1), p 38.

39 *Metco Plasma Spraying Manual*, **1993**, Metco, USA.

40 J. Wrigren, **1991**, Surf. Coat. Tech., v 45, p 263.

41 M. G. Nicholas and K. T. Scott, **1981**, Surfacing Journal, v 12, p 5.

42 W. Funk and F. Goebe, **1985**, *Thin Solid Film*, v 128, p 45.

43 B. Wielage, V. Hofmann, A. Steinhauser and G. Zimmerman, **1998**, *Wear*, v 14(2), P 136.

44 N. Y. Lee, D. P. Stinton, C.C. Brandt, F. Erdogan, Y. D. Lee and Z. Mutasim **1996**, J. Am. Cer. Soc., v 79(12), P, 3003.

45 A.Pajares, L. Wei, B.R. Lawn and C.C. Berndt., **1996**, J. Am. Cer. Soc., 79(7), p 1907.

46 R. C. Novak, **1988**, J. Gas Turbines and Power, v-110, p 110.

47 A.R. Nash, N. E. Weare and D. L. Walker, July, **1961**, J. Metals, July, p 473.

48 H. Gruner, **1984**, *Thin Solid Film*, v 118, p 409.

49 H. Eaton and R. C. Novak, **1986**, Surf. and Coating Technology ., v 27, p 257.

50 H. Eaton and R. C. Novak, Proc. Int. Conf on metallurgical Coatings, San Diego, USA.

51 K. Ramchandran and P. A. Selvarajan, **1998**, Thin Solid Film, v 315, p 149.

52 H. S. Ingham and A. J. Fabel, February, **1975**, Welding Journal, p 101.

53 S. Oki, S. Gonda and M. Yanokawa, **1998**, Proc. 15th International Thermal Spray Conference, 25 – 29th May, France, p 593.

54 A.F. Puzryakov, S. A. Levitin and V. A. Garanov, **1985**, Poroshkovaya Metallurgya, v 8 (272), p 55.

55 J. Hennaut, J. Othzemouri and J. Charlier, **1995**, Mat. Sc and Tech., 1995, v 11, p 174.

56 S. Sampath, R. A. Neiser, H. Herman, J. P. Kirkland and W. T. Elan., **1993**, J. Mat. Res., v 8(1), p 78.

57 J. Hennaut, J. Othmezouri and J. Charlier, **1995**, Mat. Sc and Tech., 1995, v11, p 174.

58 B.Elvers, S. Hawkins and G. Schultz (eds), **1990**, Ulhmann's Encyclopedia of Industrial Chemistry, v 1/16, VCH, p 433.

59 C.J. Kubel, Adv. Mat. Proc., **1990**, v12, p 24.

60 M. Codenas, R. Vijande, H. J. Montes and J. M. Sierra, **1997**, *Wear*, v 212, p 244.

61 Nolan, P. Mercer, and M. Samadi, **1998**, Surf. Engg, v11(2), p 124.

62 Y.Naerheim, C. Coddet and P. Droit, **1995**, Surf. Engg, v11(1), p 66.

63 K. Hojmrle and M. Dorfman, **1985**, *Mod. Dev. Powder. Met*., v 15(15), p 609.

64 O. Knotek, E. Lugscheder and H. Reiman, **1975**, J. Vac. Sc. Tech A, v 12(4), p 75.

65 M. Roy, C.V.S. Rao, D. S. Rao and G. Sundarrajan, **1999**, Surface Engineering, v 15(2), p 129.

66 Chuanxian, H. Bingtang , L. Huiling, **1984**, Thin Solid Film, v 118, p 485

67 J.M.Guilemay, J.M.De Paco,**1998**, Surface Engineering., v.11 (2), p 129.

68 Y. Wang, **1993**, *Wear*, v 161, p 69.

69 Y. Wang, J. Yuansheng and W. Shizhu, **1988,** *Wear*, v 128, p 265.

70 A.Tronche and P. Fauchais, **1988**, *Wear* , v 102, p 1.

71 A.A. Stuart, P. H. Shipway and D. G. McCartney, **1999**, *Wear*, v 225-229, p 789.

72 S. Economou, M. De Bonte, J.P. Celis, J. R. Roos, R. W. Smith, E. Lugscheider and A. Valencic, **1995**, *Wear*, v185, p 93.

73 U. Menne, A. Molar, M. Bonner, C. Varpoort, K. Ebert and R. Bauman, **1993,** Proc. Themal Spraying – 93, 1993, p 280.

74 M. Mohanty, R. W. Smith, M. De Bonte, J. P. Celis and E. Lugscheder, **1996,** *Wear*, v 198, p 251.

75 J. F. Li, C. X. Ding, J. Q. Huang and P. Y. Zhang, **1997**, v, p 177.

76 J. M. Cuetos, E. Fernandez, R. Vijandez, A. Rucon and M. C. Perez, **1993**, *Wear*, v 169, p 173.

77 W. Jainjun and X. Qunji, **1993**, *Wear*, v 162 – 164, p 229.

78 J. F. Lin and T. R. Li, **1990**, *Wear*, v 160, p 201.

79 A.S. Ahn and O. K. Kwon, **1999**, *Wear*, v 225 – 229, p 814.

80 W. Jainjun, X. Qunji and W. Huiling, **1992**, *Wear*, v 152, p 161.

81 S. Lathabai, M.Ottmuller , I. Fernandez, **1998**, *Wear*, v 221,p 93.

82 L.Zhou, Y. M.Gao, J.E. Zhou, Q.D.Zhou, **1994**, *Wear* , v 176,p 39.

83 A.S. Ahn and O. K. Kwon, **1993**, *Wear*, v 162 – 164, p 636.

84 T. F. J. Quinn and W. O. Winer, **1985**, *Wear*, v 102, p 67.

85 A.Y. Kim, D. S. Lim and H. S. Ahn, **1993**, J. Kor. Cer. Soc, v 30, p 1059.

86 H. S. Ahn, J. Y. Kim and D. S. Lim, **1997**, *Wear*, v 203 – 204, p 77.

87 Y. Fu, A. W. Batchelor, H. Xing and Y. Gu, **1997**, *Wear*, v 210, p 157.

88 Y. Sun, B. Li, D. Yang, T.Wang,Y. Sasaki and K. Ishii, **1998**, *Wear*, v 215, p 232.

89 Y. S. Song, J. C. Han, M.H. Park, B.H.Ro, K. H. Lee, E. S. Byun, S. Sasaki, **1998**, Proc. 15th International Thermal Spray Conference, 25th – 29th May, France, p 225.

90 M. I. Mendelson, **1978**, *Wear*, v 50, p 71.

91 *Metco Technical Bulletin on TiO_2*, **1971**, Metco Inc., NY, USA.

92 W. W. Dai, C. X. Ding, J. F. Li, Y.F. Zhang and P. Y. Zhang, **1996**, *Wear*,196, p 238.

93 N. P. Suh, **1973**, *Wear*, v 25, p 111.

94 H. So, **1995**, *Wear*, v 184, p 161.

95 T. S. Eyre, **1975**, *Wear*, v 34, p 383.

96 Halling, Principles of Tribology, The Mcmillan Press Ltd, NY, USA, **1975**.

97 Y. Guilmad, J. Denape and J. A. Patil, **1993**, Trib. Int. v 26, P 29.

98 M. G. Gee, **1992**, *Wear*, v 153, p 201.

99 R. Mcpherson, **1973**, J. Mat. Sc., v 8, P 859.

100 R. Mcpherson, **1980**, J. Mat. Sc., v 15, P 3141.

101 A.R.D.A. Lopez , K. T.Faber, **1999**, J. Am. Cer. Soc., v 82(8), p 2204.

102 H. Ono, T. Teramoto and T. Shinoda, **1993**, Mat and Mfg. Processes, v 8(4&5), p 451.

103 S. Musikant, **1991**, *What Every Engineer Should Know About Ceramics*, Marcell Dekker Inc, NY, USA.

104 R. P. Wahi, and B. Lischner, **1980**, J. Mat. Sc, v 15, p 875.

105 T. Yamamota, M. Olsson , S. Hogmark, **1994**, *Wear*, v – 174, p 21.

106 A.Lamy and T. N. Sopkow, **1990**, Proc. 3rd National Thermal Spray Conference, Long Beach, CA, USA, 20 – 25th May, p 491.

107 D. Matejka and B. Bonko, *Plasma Spraying of Metallic and Ceramic Materials*, Willey, Chichester, UK, **1989**.

108 M. A. Moore and F. A. King, **1980**, *Wear,* v 60, p 123.

109 Cheo, W. D. Kulhmann and D. M. David, **1994**, *Wear*, v 173, p 1

110 A. L. Fernandez, R. Rodriguez, Y. Wang, R. Vijande and A. Rincan, **1995**, *Wear*, v 181 – 183, p 417.

111 Y. S. Wang, S. M. Hsu and R. G. Munro, **1991**, *J. Soc. Of Tribologists and Lubri. Engg*., v 47(1), p 63.

112 Metals Handbook, ASM, Metals Park, Ohio, USA.

113 S. Atamert and J. Stekly, Microstructure, **1993**, Surf. Engg., v 9(3), p 231.

114 M. O. Price, T. A. Wolfla and R. C. Tucker, **1977**, *Thin Solid Films*, v 45, p 309.

115 M. A. Moore, **1994**, *Wear*, v 28, p 59.

116 P. L. Hurricks, **1972**, *Wear*, v 22, p 291.

117 M. G. Habsur and R. V. Miner, **1986**, Mat. Sc. Engg, v 83, p 239.

118 A. E. Spear, **1989**, J. Am. Cer. Soc., v 72, p171.

119 A. Marakawa, **1997**, Mat. Sc. Forum, v 247, p 1.

120 K. Oyoda, S. Komatsu, S. Matsumoto, Y. Moriyoshi, **1991**, J. Mat. Sc., V 26, p 3081.

121 W. Zhu, B. H. Tan and H. S. Tan, **1993**, *Thin Solid Films*, v 236, p 106.

122 P. Hollman, A. Alhelisteten, T. Bjorke and S. Hogmark, **1994**, *Wear*, v 179, p 11.

123 A. Alhelisten, *Abrasion of Hot Flame Deposited Diamond Coatings, Wear*, **1995**, v 185, p 213.

124 M. Rosso, A. Bennani, PM World Congress Thermal Spraying/ Spray Forming, 1998, p. 524.

125 H.V. Hidalgo, F.J.B. Varela, E.F. Rico, Tribol. Int. 30 (9) (1997) 641.

126 J. Ilavsky, J. Pisacka, P. Chraska, N. Margadant, S. Siegmann, W.Wagner, P.Fiala, G. Barbezat, Proceedings of the International Thermal Spray Conference, 2000, p. 449.

127 C. T. Liu and C. L. White, in High Temp. Ordered Intermettallic Alloys by C. C. Koch, C. T. Liu and N. S. Stoloff, Mat . Res. soc., 39(1985),365.

128 R. W. Chan, Load-Bearing Ordered Intermettalic Compounds- A Historical View, MRS Bulletin, 5,(1991),18.

129 S.Y.Guo, J.Li, D.S.Mao, M.H.Xu and Z.Y.Mao, Wear, V203-204, pp319, **1997.**

130 Angle, P. A**.** *Impact Wear of Materials*, (Elsevier; New York, ***1976***).

131 Tilly, G.P. "*Erosion Caused by Impact of Solid Particles*", in H. Herman (ed), Treatise on Materials Science and Technology, vol. 13:D. Scott(ed), Wear. (Academic Press: New York, **1979**) p. 287 – 320.

132 *Erosion by Liquid and Solid Impact*. (Cavendish Laboratory, University of Cambridge: Cambridge, England, **1979)**.

133 *Erosion by Liquid and Solid Impact*. (Cavendish Laboratory, University of Cambridge: Cambridge, England, **1987**).

134 Evans, A. G. "*Impact Damage Mechanism – Solid Projectile*", in H. Herman (ed.), Treatise on Materials Science and Technology, Vol. 16: C. M. Preece (ed.), Materials Erosion, (Academic Press: New York, **1979)**, p. 1 – 67.

135 *The erosion and abrasion characteristics of alumina coatings plasma sprayed under different spraying conditions* R. Westergard, L. C. Erickson, N. Axen, H. M. Hawthorne and S. Hogmark, Tribology International, Volume #1, Issue %, May ***1998***, Pages 271 – 279.

136 Tucker, R. C. Jr., *On the relationship between the microstructure and the wea characterstics of selected thermal spray coatings*. Proceeding of ITSC, Kobe, Japan, **1995**, pp. 477 – 482.

137 H. M. Hawthorne, L. C. Erickson, D. Ross, H. Tai and T. Troczynski, *The microstructurral dependence of wear and indentation behaviour of some plasma sprayed alumina coatings*. Wear 203 – 204 (1997), pp. 709 – 714.

138 Erickson, L. C., Troczynski, T., Ross, D., Tai, H. and Hawthorne, H. M., *Processing – dependent microstructure and wear – related surface properties of plasma sprayed alumina coatings*, presented to World Tribology Congress, Londan, U. K., September **1997**.

139 Erickson, L. C., Troczynski, T., Hawthorne, H. M., Tai, H. and Ross, D., *Alumina coatings by plasma spraying of monosize sapphire powders*, published in the proceedings of ITSC'98, Nice, France.

140 A.Ohmori, C. – J. Li and Y. Arata, *Influence of Plasma spray conditions on the structure of Al_2O_3 coatings*. Trans. Of JWRI 19 2 (**1990**), pp. 99 – 110.

141 F. Alonso, I. Fagoaga and P. Oregui.- "*Erosion Protection of carbon – epoxy composites by plasma sprayed coatings*", Suface & Coatings Technology, Volume 49, Issues 1 – 3, 10 Dec, **1991**, pp. 482 – 488,

142 W. Tabakoff, V. Shanov. -- "*Erosion rate testing at high temp. for turbo machinery use",* - Surface & Coatings Technologies, Vol. 76 – 77, Part I, Nov **1995**, pp. 75 – 80,

143 C. He, Y. S. Wang, J. S. Wallace and S. M. Hsu, **1993**, *Wear* , V 162 – 164, p 314.

144 O. O. Ajayi and K. C. Iudema, **1991**, *Wear*, v 124, p 307.

145 R. Mcpherson, 1989, Surf. Coat. Tech., v 39/40, p 173.

146 B.Wang, **1996**, *Wear*, v 199, p 24.

147 F.M. Hawthrone, L. C. Erickson, D. Ross, H. Tan and T. Trockzynsko, **1997**, *Wear*, v 203 – 204, p 709.

148 X. S. Zhang, T. W. Clyne and I. M. Hutchings, **1997**, Surf. Engg., v 13(5), p 393.

149 Jose Roberto Tavares Branco, Robert Gansert, Sanjay Sampath, Christopher C. Berndt, Herbert Herman-- *Solid Particle Erosion of Plasma Sprayed Ceramic Coatings*—Materials Research. Vol.7. No.1.147-153 , **2004**

150 S.B. Mishra, K.Chandra, S. Prakash, B.Venkataraman – Characterisation and Erosion Bhehaviour of a Plasma Sprayed Ni3-Al Coating on a Fe-based Superalloy – Materials Letters 59 (2005) pp 3694-3698

151 H. Chen, S.W. Lee, Hao Du, Chuan X Ding and Chul Ho Cho; " *Influence of feed stock and spraying parameters on the deposition efficiency. and microhardness of plasma sprayed zirconia coatings*" -- Materials Letter Vol 58, Issues 7 – 8, March **2004** pp. 1241 – 1245

152 B. Venkataraman – *Evaluation of Tribological Coatings* – Proc. of DAE-BRNS Workshop on Plasma Surface Engineering, BARC, Mumbai, September **2004**, pp. 217 – 235.

153 G .Lalleman – Tallaron, *Study of Microstructure and adhesion of spinelles coatings formed by plasma spraying*, Ph. D. Thesis No. 96 – 58 (**1996**) E. C. Lyon, France.

154 S. C. Mishra. K. C. Rout, P. V. Ananthapadmanabhan and B. Mills *Plasma Spray Coating of Fly Ash Pre-Mixed with Aluminium Powder Deposited on Metal Substrates.* J. Material Processing Technology **2000**. 102, 1 – 3 , pp. 9 – 13.

155 C.R.C. Lima, R.E.Trevisan. J.Themal Spray Tech. 62, **1997** , p. 199.

156 Lech Pawlowski – *The Science and Engineering of Themal Spray Coatings*, John Wiley & Sons, New York (**1995**) pp. 235.

157 S.Rajasekaran , G. A. Vijayalakshmi Pai --*Neural Networks, Fuzzy Logic And Genetic Algorithms—Synthesis and Applications* -Prentice Hall of India Pvt. Ltd. , New Delhi (**2003**)

158 V. Rao and H. Rao 'C++ Neural Networks and Fuzzy systems' BPB Publications, **2000**.

159 Levy, A. V. The erosion corrosion behavior of protective coatings, Surf. and Coat. Techn., v. 36. p. 387 – 406, **1988**.

160 Weight, I. G.; Shetty, D. K. *A Phenomenological Approach to Modelling the Erosion of WC – Co Alloy,* 7th ELSI. Paper 43.

****